SAPIENZA
UNIVERSITÀ DI ROMA

Strange baryon matter and the hyperon puzzle

Facoltà di Scienze Matematiche, Fisiche e Naturali

Corso di Laurea Magistrale in Fisica

Candidate

Federico Montereali

ID number 1647078

Thesis Advisor

Prof. Omar Benhar Noccioli

Academic Year 2020/2021

Thesis not yet defended

Strange baryon matter and the hyperon puzzle
Master's thesis. Sapienza – University of Rome

This thesis has been typeset by LaTeX and the Sapthesis class.

Author's email: montereali.1647078@studenti.uniroma1.it

A mia Madre

Contents

Introduction

Compact stars, commonly grouped as white dwarfs, neutron stars and black holes, are considered to be the final stage of stellar evolution. They are different from normal stars in two fundamental aspects. The first one is that in the compact stars, most of the nuclear fuel necessary to ignite fusion reactions leading to heat production has been consumed, so they cannot support themselves against gravitational collapse by generating thermal pressure. The hydrostatic equilibrium is obtained thanks to the pressure produced by several mechanisms, driven by quantum effects and interactions between the constituents of matter in the star interior: white dwarfs are supported by the pressure of degenerate electrons, while neutron stars by the pressure produced by both degenerate neutrons and hadronic interactions. Black holes, instead, are completely collapsed stars.

The pressure generated by strong interactions, in addition to degeneracy pressure, is necessary for the neutron star equilibrium because at the core densities it is not possible to treat neutrons as non interacting particles, as it is done for the degenerate electron gas in white dwarfs. This fact was established in 1939 by Oppenheimer and Volkoff who in their pioneering study [1] showed that the mass of a star composed of noninteracting neutrons cannot exceed $\sim 0.8 M_\odot$, where $M_\odot$ indicates the mass of the sun. This limit mass, the analogue of the Chandresakhar mass of white dwarfs [2], turns out to be in complete disagreement with any observed neutron star masses, that are much larger (typically $\sim 1.4 M_\odot$).

The second different aspect is their extremely small size: comparing them to normal stars of similar mass, compact objects have much smaller radii and much stronger surface gravitational potentials. As a consequence, general relativity has a considerable effect in determining their structure, especially for neutron stars and black holes, for which the effects of space-distortion become large. Instead white dwarfs can be described, as normal stars, using Newton gravity with atomic and low-energy nuclear physics under conditions observable in laboratory.

Compact objects span an enormous density range. The typical interval of white dwarfs and neutron stars is $10^4 - 10^{15}$ g/cm^3. To describe the internal region of a compact star, where the density is greater than 2.67×10^{14} g/cm^3, that is the value of central density of atomic nuclei, i.e. the largest density observed on earth under ordinary conditions, it is necessary to require a significant amount of extrapolation of the available empirical data on the properties of strongly interacting matter. It is important to note that all four fundamental interactions (gravitation, electromagnetism, strong and weak nuclear forces) play a role in compact stars that are an unparalleled laboratory for studying the matter under extreme conditions of temperature and density.

Neutron stars are thought to be the leftover of the gravitational collapse, following the explosion of a supernova whose progenitor was a star with mass larger than $8M_{\odot}$, and their true nature is not yet completely understood. The core of neutron stars is usually considered as a uniform fluid of neutron-rich nuclear matter in equilibrium with respect to the weak interaction (β-stable matter). However, due to the extreme conditions of pressure and density in the core of such stars, numerous particle processes, ranging from appearance of exotic particles to quark deconfinement, can happen with considerable impacts on the evolution and global properties of neutron stars.

Hyperons, baryons with strangeness content, may appear in the inner core of neutron stars around twice normal nuclear matter density. Contrary to terrestrial conditions, where hyperons are unstable and decay into nucleons through the weak interaction, in the degenerate dense matter forming the core, Pauli blocking prevents hyperons from decaying and the equilibrium conditions in the star can make the inverse process happen. At such densities, the nucleon chemical potential overcomes the nucleon-hyperon mass difference and the conversion of nucleons into hyperons becomes energetically favorable.

The theoretical analysis and the description of the properties of hyperon stars depends strongly on the model chosen to describe the interparticle interactions and, consequently, different equations of state (EOS), i.e. the functional dependence of pressure on total energy density, can be obtained. They are the basic input quantities for solving Einstein's field equations that describe the structure and the hydrostatic equilibrium configurations of neutron stars. In particular case of spherical, static and relativistic stars, the Einstein's equations take a specific form, the Tolman-Oppenheimer-Volkoff (TOV) equations.

The replacement of most energetic neutrons by massive, slowly moving hyperons, relieves the Fermi pressure exerted by the baryons and makes the EOS softer. Furthermore, the presence of exotic particles such as hyperons in the core has important impact on other neutron star properties, such as their cooling and structural evolution and also the mass-radius relation, provided by solving the TOV equations.

Once the equation of state are softened, the maximum neutron star mass is reduced from the typical limit around $2M_{\odot}$ to $\sim 1.4M_{\odot}$ that is incompatible with observations. This is the *hyperon puzzle*, which has become more fascinating and difficult to solve due the recent measurements of the unusually high masses of the millisecond pulsars PSR J1903+0327 ($1.667\pm0.021M_{\odot}$), PSR J1614−2230 ($1.97\pm0.04M_{\odot}$), and PSR J0348+0432 ($2.01\pm0.04M_{\odot}$).

The search for a solution is focused on finding a mechanism that could make the EOS stiffer and therefore the maximum mass compatible with the current observational limits.

Since the pioneer work [3] of Ambartsumyan and Saakyan (1960) the presence of hyperons in neutron stars has been studied by many authors using either relativistic or non-relativistic approaches of hyperonic matter. Building a model to implement equations of state in the right way is very difficult for both the complexity of the interactions and the approximations necessarily implied in the theoretical description of quantum mechanical many-body systems, since the number of baryons in hyperon stars is of the order of 10^{57}.

The traditional approach to this latter problem is based on nonrelativistic two-body

interaction, but it is intrinsically limited to density values for which the nonrelativistic approximation is applicable, i.e. when the nucleon Fermi energies are much smaller than the corresponding masses, and fails to fulfill the constrain of casuality, as it leads to predict a speed of sound in matter that exceeds the speed of light at large density. Moreover, experimental data providing information on hyperon-nucleon (YN) and hyperon-hyperon (YY) interactions are few and not very accurate.
The alternative approach to the nuclear many-body problem involves the formulation of an effective relativistic field theory of interacting hadrons, that respects the casuality limit by construction. This approach is based on a somewhat semplified dynamics and on the mean field approximation that is strictly valid only in the limit of infinite density. In addition, several of the parameters entering these models cannot be fully constrained by the available experimental data.
This theory is defined as effective because even if the fundamental theory of strong interactions, the quantum chromodynamics (QCD), is known, its complexity and the nonperturbative nature make it unusable at the typical scale of astrophysical situations and so the description of the forces acting between particles in hyperon stars cannot be based on the elementary degrees of freedom of QCD, quarks and gluons, but it must be realized in terms of hadronic degrees of freedom, baryons and mesons.
The thesis is structured as follows. In chapter 1 we briefly describe the evolutionary stages of neutron stars and their internal structure. In chapter 2, we first review the main properties of nuclear matter and then we intoduce the relativistic mean field theory in order to evaluate the equation of state describing the stellar matter. The model treated in this work is the $\sigma\omega\rho$ model, which in this chapter includes only nucleons. In chapter 3 we discuss the generalization of this model to incorporate strange baryons. This is done only after analyzing in detail the chemical equilibrium and charge neutrality conditions that must be satisfied in the core of the neutron stars at supernuclear density so that hyperons appear. In chapter 4 we examine the hydrostatic equilibrium of a star in the Newtonian case and its generalization in the theory of General Relativity. This allows us to obtain the last necessary tool to investigate how the presence of hyperons can modify the main properties, such as the limiting mass, of a neutron star: the TOV equations. The results of the numerical calculations of the equation of state and then of the TOV for the case of a hadronic star consisting only of nucleons and that in which hyperon Λ is also present, are reported and compared in the chapter 5. Lastly, in chapter 6 we expose our conclusions.
In this work we have used a system of units in which $\hbar = h/2\pi = c = 1$, where h is the Planck's constant and c is the speed of light.

Chapter 1

Evolution and structure of neutron stars

The existence of neutron stars is said to have been first discussed by Bohr, Landau and Rosenfeld shortly after the discovery of the neutron in 1932. In 1934, Baade and Zwicky first suggested that a neutron star may be the leftover of the gravitational collapse, following a supernova explosion. Finally, in 1968 the newly observed pulsars, radio sources blinking on and off at a constant frequency, were identified with rotating neutron stars.
Stars begin to form inside relatively dense concentrations of gas, composed basically of hydrogen molecules, and dust known as *molecular clouds*. The cold temperatures and high densities of these clouds allow gravity to overcome thermal pressure and start the gravitational collapse that will form a star, that at this stage is called *protostar*.
As the protostar forms, loose gas falls into its center. The infalling gas releases kinetic energy in the form of heat and the temperature and pressure in the center of the protostar goes up. During the initial collapse, protostar is transparent to radiation and the collapse proceeds fairly quickly. As the density increases, the cloud becomes more and more opaque, and the energy released cannot be efficiently radiated away. Consequently, the temperature also increases and eventually it becomes enough ($\sim 6 \times 10^7$ K) to ignite the nuclear reactions turning hydrogen into helium

$$\begin{aligned} p + p &\rightarrow {}^2H + e^+ + \nu + 0.4\,\text{MeV}, \\ e^+ + e^- &\rightarrow \gamma + 1.0\,\text{MeV}, \\ {}^2H + p &\rightarrow {}^3He + \gamma + 5.5\,\text{MeV}, \\ {}^3He + {}^3He &\rightarrow {}^4He + 2p + 26.7\,\text{MeV}. \end{aligned} \tag{1.1}$$

These fusion reactions are all exothermic and the energy released in the form of kinetic energy of the produced particles provides the pressure necessary to balance the gravitational force and avoid the collapse. The protostar has now joined the *main sequence* of stars. The star will spend most of its luminous life in this state of suspended collapse as it burns its large store of hydrogen, slowly radiating energy from its surface.
Once all of the hydrogen is converted to helium, the core stops producing heat, the

internal pressure cannot be sustained and the contraction produced by gravitational attraction resumes. The core collapses on itself and a further increase of the temperature occurs. This increased core temperature cause helium to fuse into carbon in the reactions:

$$\begin{aligned} {}^4_2He + {}^4_2He &\rightarrow {}^8_4Be + \gamma \\ {}^4_2He + {}^8_4Be &\rightarrow {}^{12}_6C + \gamma. \end{aligned} \tag{1.2}$$

This fusion releases more energy than hydrogen-helium fusion, causing an increase in radiation pressure. This increase pushes matter outwards, thus expanding the star. As the star expands its surface cools and becomes redder, a *red giant* is formed.
When the available He begins to run out, the carbon core, surrounded by an envelope composed of the remaining helium, is no longer able to resists the pressure of the gravitational force and starts a new collapse reducing its size.
The evolutionary stages starting from this phase depend strongly on the mass value of the object.
If the mass of the progenitor is in the range $8M_\odot < M < 20 - 30M_\odot$ with $M_\odot = 1.989 \times 10^{33}$ g, nuclear processes are able to burn elements heavier than carbon and exothermic nuclear reactions can proceed all the way to ${}^{56}Fe$, which is the most stable element in nature. Indeed, no element heavier than ${}^{56}Fe$ can be generated by fusion of lighter elements through exothermic reactions.
The process which produces ${}^{56}Fe$ starts with silicon burning, and goes this way:

$$\begin{aligned} {}^{28}Si + {}^{28}Si &\rightarrow {}^{56}Ni + \gamma, \\ {}^{56}Ni &\rightarrow {}^{56}Co + e^+ + \nu_e, \\ {}^{56}Co &\rightarrow {}^{56}Fe + e^+ + \nu_e. \end{aligned} \tag{1.3}$$

As the iron core forms the pressure provided by nuclear burning is able to maintain the star in equilibrium. However, there are several processes which tend to destabilize the star. The most efficient are:

- Neutronization: the high mass densities reached in the core provide the electron capture by protons, also known as inverse β-decay, with a production of a large number of neutrinos:

$$e^- + p \rightarrow n + \nu_e. \tag{1.4}$$

  These neutrinos are added to those already generated in the silicon burning reactions (1.3) and, by interacting with matter very weakly, they diffuse from the core to the surface and leave the star, subtracting energy from the core.

- Photodisintegration: in the reaction (1.3) photons are produced. At temperatures of the order of 10^{10} K, the number of high energy photons (>8 MeV) is sufficient to disintegrate the iron nuclei

$${}^{56}F + \gamma \rightarrow 13\,{}^4He + 4n. \tag{1.5}$$

  This is an endothermic process which subtracts further energy to the core and, in addition, produces a large number of neutrons.

Due to the combined effect of above mechanisms, when the mass exceeds the Chandrasekhar limit, the internal pressure gradient can no more balance the gravitational attraction and the core collapses, reaching densities typical of atomic nuclei, $\rho_0 \sim 2.7 \times 10^{14}$ g/cm^3, in a fraction of a second. At this stage the core behaves as a giant nucleus, composed mainly of neutrons with a small fraction of electrons and protons. At such density the repulsive forces between neutrons and the degeneration due to the Pauli exclusion principle provide the necessary pressure to compensate the gravitational force. The nucleus becomes so incompressible that infalling matter bounces back producing a violent shock wave that ejects, in a spectacular explosion, most of the material external to the core in the outer space. This phenomenon is called *supernova explosion*. In this explosive phase, nucleosynthesis of elements heavier than ^{56}Fe is believed to occur.
The hot collapsed core or *protoneutron* star, with temperature of tens of MeV, loses its trapped neutrinos over a interval of some seconds and cools to an MeV or less. At that point, the collapsed core has reached its equilibrium composition of neutrons, protons, hyperons, leptons and possibly quarks. Thus a *neutron star*, surrounded by a nebula, is born.

1.1 Internal structure of neutron star

According to experimental observations and theoretical developments, the interior of a neutron star can be modeled, as shown in figure (1.1), as a sequence of layers of different composition and thickness surrounding an innermost core. Proceeding from the exterior, the mass density ρ increases more and more going towards the center. We first encounter an *outer crust*, ∼0.3 km thick, an *inner crust*, ∼0.5 km thick, and a *core* extending over about 10 km.

The theoretical description of matter in the outer and inner neutron star crust

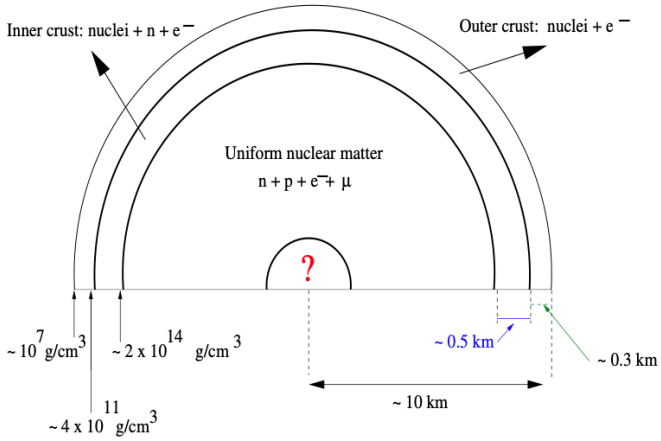

Figure 1.1. Schematic illustration of a neutron star cross section (not in scale).

will be outlined in the following sections, while the regions of core, corresponding to nuclear and supernuclear density, will be briefly introduced and then accurately described in chapters 2 and 3.

1.1.1 The outer crust

The matter density ranges from $\sim 10^7$ g/cm^3 to the neutron drip density $\rho_{drip} = 4 \times 10^{11}$ g/cm^3.
It is composed of electrons and fully ionized atoms. The ions form a Coulombian solid arranged in a Body Centered Cubic (BCC) lattice. Proceeding towards the center, as matter density increases the large kinetic energy of the relativistic electrons shifts the energy balance, favouring inverse β-decay (1.4) that leads to the appearance of new nuclear species through sequences like

$$Fe \rightarrow Ni \rightarrow Se \rightarrow Ge. \tag{1.6}$$

This process is called *neutronization* because the resulting nuclide is always richer in neutron content that initial one.
The number of nucleons A and protons Z is determined by the equilibrium configuration between the electron capture (1.4) and the β decays allowed at any density. Taking into account the internal nuclear forces of ions and phenomenological observations, at equilibrium, A is approximately an increasing function of ρ and Z depending on A according to:

$$Z \simeq 3.54\, A^{1/2}. \tag{1.7}$$

Since the number of protons grows with the root of the number of nucleons, as matter density increases, the nuclei of the outer crust are increasingly massive and neutron-rich. In this region the pressure is mainly provided by the degenerate electron gas. At $\rho = \rho_{drip}$ all bound states available in the nuclei for neutrons are filled. Neutrons can no longer live bound to the nuclei and start leaking out (neutron drip).
The matter properties in this region can be obtained directly from nuclear data. The importance of this region lies in the fact that any physical information on the central core must pass through and interact with the crust before it is revealed.

1.1.2 The inner crust

In this region the density ranges between ρ_{drip} and the nuclear $\rho_0 = 2.67 \times 10^{14}$ g/cm^3. At ρ_{drip} the ground state corresponds to a Coulomb lattice of ^{118}Kr nuclei, having proton to neutron ratio $\sim$0.31 and a slightly negative neutron Fermi energy, sourrended by a degenerate electron gas that ensures charge neutrality. As density increases, the electron fraction decreases more and more due to electron capture and neutron fluid plays an increasingly important role in maintaining equilibrium pressure.
At these densities, following the neutron drip, the ground state corresponds to a mixture of two phases: matter consisting of neutron rich nuclei (NRM), with a density ρ_{NRM} comparable to ρ_0, and a neutron gas (NG) of density ρ_{NG}.
Thus, the details of the ground state of matter in inner crust are specified by the densities of the two phases, ρ_{NRM} and ρ_{NG}, which determines the fraction of volume each phase occupies, the proton to neutron ratio of the matter in the NRM, and the geometrical properties of the structures that are formed by the two phases. These structures strongly depend on surface effects at the interface between different phases.

Recent studies suggest that at densities $\rho_{drip} \lesssim \rho \lesssim 0.35\,\rho_0$ the matter in NRM phase is arranged in spheres surrounded by the NG. For higher densities the separation between spheres decreases up to the touching limit. As a consequence, for $0.35\,\rho_0 \lesssim \rho \lesssim 0.5\,\rho_0$ the spheres merge, forming bar-type structures, and for $0.5\,\rho_0 \lesssim \rho \lesssim 0.56\,\rho_0$ the bars merge to form slab-type structures. For larger densities, the merged nuclei of NRM become a uniform fluid, with increasingly smaller contributions of NG.
When the density reaches the nuclear density ρ_0 the two phases are no longer separated and form a homogeneus fluid of neutrons, protons and electrons.
Models that describes the inner crust are based on extrapolations of the available empirical information, as the extremely neutron rich nuclei appearing in this density regime are not observed on earth.

1.1.3 The core

For $\rho > \rho_0$ in the so-called *outer core* of the neutron star, according to all models of EOS based on hadronic degrees of freedom, matter is composed mainly of neutrons, with the admixture of a small number of protons and electrons in β-equilibrium, i.e. in equilibrium with respect to the neutron β-decay

$$n \to p + e^- + \overline{\nu}_e\,, \tag{1.8}$$

and to the inverse β-decay (1.4). At any given density the fraction of protons and leptons is determined by the requirements both of this equilibrium and charge neutrality.
It should be stressed that the main contribution to the pressure in the core comes from neutrons and, since they are more massive than electrons, the total energy is also mostly provided by neutrons themselves. However, the equilibrium pressure is not produced only by neutrons but also by hadronic interactions, since at the core densities it is not possible to treat neutrons as noninteracting particles.
At these high densities several processes may develop. For instance, when electrons have kinetic energies exceeding the electron-muon mass difference, the process of conversion of neutrons into muons is energetically favorable. At even higher densities, $\rho \gtrsim 2\,\rho_0$, in the region called *inner core*, other species of particles may form but the composition of this region strongly depends on the theoretical model chosen to describe it. The main hypotheses are three. The first one is the hyperonization of matter predicts the appearance of strange baryons, such as Σ and Λ, produced in weak interaction processes thanks to the high chemical potentials of neutrons and electrons. The second one is the appearance at $\rho \sim 2 - 3\,\rho_0$ of π and K mesons that, being bosons, are not subjected to Pauli's exclusion principle and may form a Bose-Einstein condensate. The last one is the phase transition of matter, at $\sim 10^{15}$ g/cm^3, in which quarks are no longer confined to hadrons and coexist free with a small fraction of electrons.
In this work we will examine the first hypothesis that will be discussed in detail in Chapter 3, where a more complete explanation of chemical equilibrium that characterizes this region will be also treated.

Chapter 2

Physics of neutron star matter

In this Chapter, after reviewing the main properties of nuclear matter, the relativistic mean field theory employed to study the structure of neutron stars is presented.
In order to describe theoretically the dense and superdense matter of neutron stars, it is essential to remark what is known empirically about bulk nuclear matter. In practice this knowledge concerns the properties of symmetric nuclear matter at saturation density, at which the pressure is zero and the matter would remain static if not disturbed.
The body of data on nuclear masses from the nucleon-nucleon interaction can be used to constrain the density dependence predicted by theoretical models of uniform nuclear matter at zero temperature limit, that is fully justified, as the typical temperature of the neutron star interior is $\sim 10^9$°K~ 0.1 MeV, to be compared to nucleon Fermi energies of tens of MeV.
It is important to establish a relation between the theory and the properties near normal nuclear matter density because this allows to constrain the equation of state and control that the theoretical extrapolation to higher density is correct in the vicinity of saturation. The dependence of the properties of neutron stars, arising from the structure of the hadronic matter of which they are made, can therefore be related to nuclear matter properties and their uncertainties.
In equilibrated hadronic matter, at densities several times that of normal nuclear matter, the nucleon Fermi energy is sufficiently large that it is energetically favorable for some nucleons transform to heavier and strange baryons through the electroweak interaction.
The empirical information for the strange matter at these extreme densities is very scarse though they are the object of current and planned experimentation in the field of relativistic nuclear collisions. Astrophysical and gravitational wave observations of neutron stars will also provide important information. It is not possible to control this sector of the theory by ground-state properties of hadronic matter because only the nucleons populate that state. Even hyperons, mainly just the Λ occur in few hypernuclei and populate matter only at high density no affecting the ground-state properties. Consequently, considerable uncertainly surrounds the effect of hyperons on the properties of neutron stars, but nevertheless, some constraints on their couplings can be obtained.

2.1 General nuclear matter properties

The basic property of nuclei or nuclear matter is that they are saturated systems. This derives from the short range of the nuclear force and the Pauli principle [4]. A nucleon may only interact strongly with a fixed number of its nearest neighbors and next-nearest neighbors. If a further nucleon is added, only the nuclear volume becomes larger, not the binding energy per nucleon and this defines a saturated system. Moreover, since the mean free path of the nucleon is too much larger than the nucleon size, the nucleus can be considered as composed of independent nucleons moving in a mean field.
There are two main features of stable nuclei, that can be obtained experimentally. The first one is that the charge density is nearly constant whitin the nuclear volume, its value being roughly the same for all stable nuclei, and drops from $\sim 90\%$ to $\sim 10\%$ of the maximum over a distance $R_T \sim 2.5$ fm, independent of mass number A. It can be parametrized in the form

$$\rho_{ch}(r) = \rho_0 \frac{1}{1 + e^{(r-R)/D}} \tag{2.1}$$

where $R = r_0 A^{1/3}$ is the nuclear radius, with $r_0 = 1.07$ fm, estimated by the scattering of low-energy electrons from nuclei, and $D = 0.54$ fm. It is to be noted that the nuclear charge radius is proportional to $A^{1/3}$, implying that the nuclear volume increases linearly with the mass number A.
The second very important feature is the positive binding energy per nucleon and its dependence on A and atomic number Z, that can be parametrized according to the *semiempirical mass formula*

$$\frac{B(Z,A)}{A} = \frac{1}{A}[a_V A - a_s A^{2/3} - a_c \frac{Z^2}{A^{1/3}} - a_A \frac{(A-2Z)^2}{4A} + \lambda a_p \frac{1}{A^{1/2}}]. \tag{2.2}$$

The first term in the square brackets, proportional to A, is called *volume term* and describes the bulk of energy of nuclear matter which results from the mutual attraction between nucleons. The second term, proportional to the nuclear radius squared, is associated with the surface energy. This contribution arises because nucleons at the surface interact in a repulsive way with fewer neighbors and so feel less attraction than those in the interior. The third one accounts for the Coulomb repulsion between Z protons and uniformly distributed within a sphere of radius R. The fourth term, that is named *symmetry energy* is required to describe the experimental observation that stable nuclei tend to have the same numbers of neutrons and protons. Moreover, even-even nuclei, i.e. nuclei having even Z and even A-Z, tend to be more stable than even-odd or odd-odd nuclei. This property is accounted for by the last term in the above equation, where λ=-1, 0 and +1 for even-even, even-odd and odd-odd nuclei, respectively. All contributions provided by these terms to total binding energy per nucleon are shown in Fig. 2.1.
In the thermodynamical limit, i.e. considering large A and infinite volume, the only term surviving in the case Z=A/2 is the first term. Consequently, the coefficient a_V can be identified with the binding energy per particle of *symmetric nuclear matter*, an ideal uniform system consisting of equal number of protons and neutrons coupled by strong interactions only.

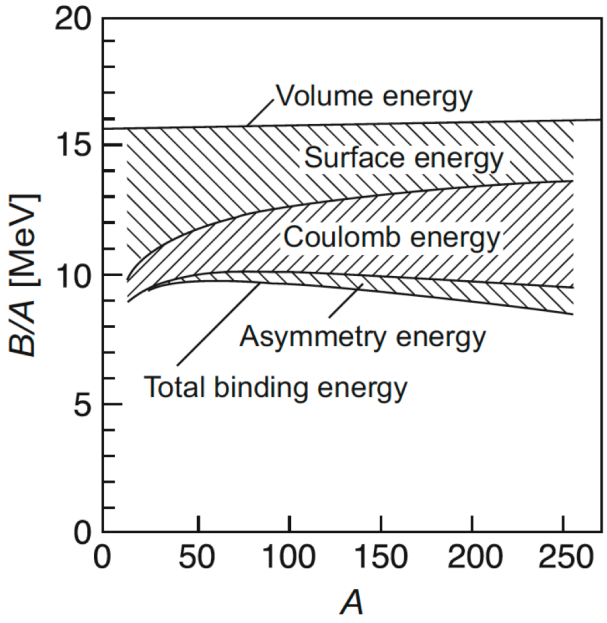

Figure 2.1. Binding energy per nucleon B/A trend in function of mass number A for the several terms of eq. 2.2. The volume energy is practically constant and with the other energy contributions defines the behavior of the total binding energy shown.

The equilibrium density, of such a system, n_0, can be obtained exploiting saturation of nuclear densities, i.e. the fact that the central density of atomic nuclei, measured by elastic electron-nucleus scattering, does not depend upon A for large A, as shown in Fig. 2.2.

The empirical equilibrium properties of symmetric nuclear matter are [5]

$$e_0 = \left(\frac{B}{A}\right)_{n=n_0} \sim -16\,\mathrm{MeV}, \quad \mathrm{n}_0 \sim 0.16\,\mathrm{fm}^{-3}. \tag{2.3}$$

The binding energy per nucleon and nucleon number density at saturation are the two minimal constraints to which any theory of matter that is intended to describe neutron stars should be anchored. In any case, some of the additional important constraints can be obtained.

The first of these quantities is the symmetry energy, i.e. the fourth term of equation 2.2, that has been briefly discussed earlier. To understand the importance of this property it is necessary to consider the nuclear medium as a quantum degenerate Fermi gas, in which all energy levels are occupied separately by neutrons and protons up to the Fermi energy $k_F^2/2m$ with $k_F^2 = (3\pi^2 n)^{1/3}$, according to Pauli's exclusion principle. When more nucleons are added, they occupy the higher energy levels, increasing the total energy of the medium and decreasing the binding energy. If there is an unequal number of protons and neutrons, usually there are more neutrons than protons, their Fermi energies are also different.

In that case, the role of the simmetry energy contribution to the total binding energy is to assure that protons and neutrons have the same Fermi energy. Thus, the symmetry energy provides for an equilibrium between proton and neutron number,

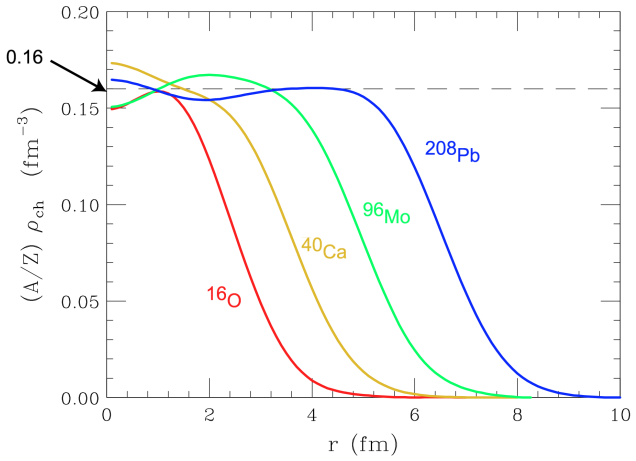

Figure 2.2. Saturation of central nuclear densities measured by elastic electron-nucleus scattering.

vanishes for $n_p = n_n$, and lowers the total binding energy by increasing the difference $n_p - n_n$. The empirical value of the symmetry energy coefficient at the saturation density, as for the binding energy per nucleon and nucleon number density, is well known [5]

$$a_{sym} = 31.6 \pm 2.66\,\text{MeV}. \tag{2.4}$$

In the vicinity of the equilibrium density $e = B/A$ can be expanded according to

$$e(n) \approx e_0 + \frac{1}{2}\frac{K}{9}\frac{(n-n_0)^2}{n_0^2}, \tag{2.5}$$

where

$$K = 9n_0^2\left(\frac{\partial^2 e}{\partial n^2}\right)_{n=n_0} = 9\left(\frac{\partial P}{\partial n}\right)_{n=n_0} \tag{2.6}$$

is the compression modulus, which defines the slope of the pressure at saturation density and multiplied by 9. This is another relevant contact with empirical knowledge and can be extracted from the measured excitation energies of nuclear vibrational states. Due to difficulties implied in the analysis of these experiments, however, empirical estimates of K have a rather large uncertainty, and a range from ∼220 MeV, corresponding to more compressible nuclear matter, i.e. to a *soft* EOS, to ∼260 MeV [5], corresponding to a *stiff* EOS. The stiffness directly influences the maximum mass of the neutron star sequence, that will be studied in the next chapters, belonging to the equation of state.

The last important quantity in the study of nuclear matter properties is the nucleon effective mass m_N^*, which results from the mass defect of the nucleon due to the interaction with its nearest neighbors. Experimentally, it is possible to determine its value by measuring the density of states of the nucleon and the single-particle energy levels in nuclei. However, like the compression modulus, a precise value of the nucleon effective mass is not known at present. It is only possible to establish a validity range at saturation density and for symmetric matter [6], that is $m_N^*/m \approx 0.7$ to

0.8.
Starting from these constraints, we can build theoretical models that reproduce the empirical data of the physical properties in nuclear medium, as accurately as possible, and make quantitative and qualitative predictions on the physical behavior of the nuclear matter at extreme conditions, which is not yet known.

2.2 Relativistic mean field theory

In this section we will discuss the relativistic mean field theory, in particular the σ-ω-ρ model, which will be used in this work for the study of hadronic stars. The choice to use this approach over that based on the many-body theory is due to the different problems, which will be discussed briefly, of this latter model in describing the matter at the high densities present in neutron stars.
The first model of many-body theory was developed by Brueckner, Bethe and Goldstone [7] in order to discover if the properties of nuclear matter can be correctly found from the two-nucleon interaction (NN), mediated by meson exchange, as it is determined from scattering experiment. However, considering the interaction of nucleons at ever higher density, the proximity of other nucleons must involve the simultaneous interaction of more than two. It is therefore clear that other elements, such as three-body interaction, must be taken into account in order to reproduce the known properties of matter as correctly as possible. Although the saturation point and the binding energy are in good agreement, the symmetry energy coefficient and compression modulus, that are important for extrapolating to denser and isospin asymmetric neutron star matter, are not.
Moreover, the application of the the many-body model to calculate the limiting mass of neutron stars is quite challenging since the equation of state becomes acausal before the central density of the limiting mass star is attained. This is quite common in the nonrelativistic approach but noncausality is not the only problem.
In fact, nucleons as the entities we know in vacuum or in normal nuclei with their usual properties and interactions at such densities seems not to be viable. From all of the above discussion, it appears to us that the many-body model is not suitable for transcribing what is know about the vacuum interaction to the densities found in neutron stars.
There is also a relativistic extension of Brueckner theory and it is the Dirac-Brueckner method. This method employs the Dirac equation for single-particle motion in nuclear matter and a one-boson-exchange potential for the interaction [8]-[9]. Nuclear matter properties seem to be better under control, but the same problems in dealing with dense matter, as discussed above, exists and its numerical solution is very complicated, so they cannot be applied to finite nuclei.
From all these considerations, the choice of the relativistic mean field (RMF) theory seems to be the most suitable and can provide a causal extrapolation to higher density.
In principle, relativistic quantum field theory provides a well defined theoretical framework in which relativistic effects can be taken into account in a fully consistent fashion but due to the complexity and non perturbative nature of the strong interaction, this initial approach to the nuclear many problem, based on the QCD

lagrangian, involves prohibitive difficulties.
The fact that most of the time nucleons in nuclear matter behave as individual particles interacting through boson exchange suggests that the fundamental degrees of freedom of QCD, quarks and gluons, may indeed be replaced by nucleons and mesons, to be regarded as the degrees of freedom of an effective field theory, in which the lagrangian describing the interactions between elementary constituents is replace with properly constructed effective interactions.
In this section we will describe a simple model in which nuclear matter is viewed as a static and uniform system of A bound nucleons (Z protons and N neutrons) moving in a volume V, which is assumed to be very large so that the surface effects can be neglected. Each nucleon field is represented by a Dirac-spinor as an isospin doublet state of proton and neutron, interacting through exchange of a scalar and two vector mesons, called σ, ω and ρ, respectively.

2.2.1 σ-ω-ρ model

The σ-ω-ρ model is an effective theory and represents one of the evolutions of the model originally proposed by Walecka in 1974 [10], the σ-ω model. In this model, the exchange of ω and σ mesons between nucleons is known to provide the short-range repulsion and intermediate-range attraction in the nucleon-nucleon potential. The extension of this model includes the self-interaction terms of the scalar field σ and the introduction of a second vector meson ρ. The reasons of these two additional elements of the theory come from different considerations. First, the original model provides a good agreement with the empirical values of saturation density and binding energy, but not of the compression modulus, the effective nucleon mass and the symmetry energy at saturation, that are brought under control considering the σ self-interaction terms, introduced by Boguta and Bodmer [11]. Second,the σ meson is isoscalar-scalar and the ω meson is isoscalar-vector, i.e. both are neutral with total spin J = 0 and 1, respectively. Consequently, they do not have isospin-dependence in the Walecka Lagrangian density, and therefore they do not contribute in the asymmetry energy. To obtain the empirical value (2.4), it is necessary to introduce the ρ meson into the Lagrangian density of the theory, which is an isovector meson with unitary charge and couples to the isospin density, i.e. to the difference between the density of protons and neutrons, $n_p - n_n$.
It should be noted that, although the σ-ω-ρ model provides a satisfactory description of the structure of nuclei, this quantum field theory provides good results at large distances but breaks down at short distances, because it treats mesons and baryons as elementary degrees of freedom and at short distances quarks and gluons manifest themselves.
The determination of dynamics is however ruled by the general properties of the QCD, the theory of elementary degrees of freedom of quarks and gluons, and its symmetries. The interaction must be invariant under the group of QCD transformations and, in addition, the lagrangian form must allow to reproduce the empirical properties of nuclear matter at the saturation point. For this reason, the coupling constants and the meson masses are treated as free parameters, to be adjusted on the basis of the experimental data of nuclear matter.

The basic element of the σ-ω-ρ model is the lagrangian density

$$\mathcal{L} = \mathcal{L}_N + \mathcal{L}_M + \mathcal{L}_{int}, \tag{2.7}$$

where $\mathcal{L}_N$, $\mathcal{L}_M$, and $\mathcal{L}_{int}$ describe free nucleons and mesons and their interactions, respectively. The dynamics of the free nucleon field is dictated by the Dirac lagrangian

$$\mathcal{L}_N = \overline{\psi}(x)(i\partial_\mu\gamma^\mu - m_N)\psi(x) \tag{2.8}$$

where m_N is the averaged nucleon free mass and the nucleon field combines the two four-components Dirac spinors describing proton and neutron, $\psi(x) = \binom{p}{n}$. The meson lagrangian reads

$$\begin{aligned}\mathcal{L}_M = \mathcal{L}_\sigma + \mathcal{L}_\omega + \mathcal{L}_\rho = \frac{1}{2}\partial_\mu\sigma(x)\partial^\mu\sigma(x) \\ - \frac{1}{2}m_\sigma^2\sigma(x) - \frac{1}{4}F^{\mu\nu}(x)F_{\mu\nu}(x) + \frac{1}{2}m_\omega^2\omega_\mu\omega^\mu \\ - \frac{1}{4}B_{\mu\nu}(x)B^{\mu\nu}(x) + \frac{1}{2}m_\rho^2\rho_\mu\rho^\mu\end{aligned} \tag{2.9}$$

where

$$\begin{aligned}F_{\mu\nu} = \partial_\nu\omega_\mu - \partial_\mu\omega_\nu \\ B_{\mu\nu} = \partial_\nu\rho_\mu - \partial_\mu\rho_\nu,\end{aligned} \tag{2.10}$$

$\omega_\mu(x)$, $\rho_\mu(x)$ and $\sigma(x)$ are the vector and scalar meson fields, respectively, and m_ω, m_ρ, m_σ are the corresponding masses.
Lastly, the interaction lagrangian is defined by requiring that, besides being a Lorentz scalar, $\mathcal{L}_{int}(x)$ gives rise to statical potentials in the nonrelativistic limit. It reads

$$\begin{aligned}\mathcal{L}_{int} = -g_\omega\overline{\psi}(x)\gamma^\mu\omega_\mu\psi(x) - \frac{1}{2}g_\rho\overline{\psi}(x)\gamma^\mu\boldsymbol{\tau}\cdot\boldsymbol{\rho_\mu}\psi(x) \\ + g_\sigma\overline{\psi}(x)\sigma(x)\psi(x) - \frac{1}{3}\frac{g_\sigma^3}{G_3}\sigma^3(x) - \frac{1}{4}\frac{g_\sigma^4}{G_4}\sigma^4(x)\end{aligned} \tag{2.11}$$

where g_σ, g_ω, g_ρ are the coupling costants of the mesons σ, ω and ρ. The vector $\vec{\tau}$ components are the Pauli's matrices acting on bidimensional isospin space. The parameter G_3, of GeV^{-1} dimension, and that adimensional G_4 describe the self-interactions of σ as they are introduced by Boguta and Bodmer [11].
The terms $g_\sigma\overline{\psi}(x)\sigma(x)\psi(x)$ and $-g_\omega\overline{\psi}(x)\gamma^\mu\omega_\mu(x)\psi(x)$ identify medium range attraction and short range repulsion, respectively; the coupling with vector meson $\rho(x)$ defines the isospin-dependence of lagrangian density and provides asymmetry energy contribution. In fact, as briefly introduced at the beginning of this section, the vertices of interaction with the isoscalar fields $\omega(x)$ and $\sigma(x)$ do not contain operators that act on the two-dimensional space of the isospin and do not mix the components of the isospinor of the nucleon. These Lagrangian terms are separable into two contributions only dependent on proton or neutron fields and therefore do not contribute to asymmetric energy, that instead is related to the difference $n_p - n_n$ that can only be expressed by those couplings with mixed terms that contain at the same time spinors $\psi_p(x)$ and $\psi_n(x)$.

The equations of motion for the fields follow from the Euler-Lagrange equations associated with the lagrangian density of Eq. (2.7). The scalar field satisfies

$$\partial_\mu \partial^\mu \sigma(x) + m_\sigma^2 \sigma(x) = g_\sigma \overline{\psi}(x)\psi(x) - \frac{g_\sigma^3}{G_3}\sigma^2(x) - \frac{g_\sigma^4}{G_4}\sigma^3(x) \tag{2.12}$$

while the vectors fields

$$\begin{aligned} \partial_\mu F^{\mu\nu}(x) + m_\omega^2 \omega^\nu(x) &= g_\omega \overline{\psi}(x)\gamma^\nu \psi(x) \\ \partial_\mu B^{\mu\nu}(x) + m_\rho^2 \vec{\rho}^{\,\nu}(x) &= \frac{1}{2} g_\rho \overline{\psi}(x)\gamma^\nu \vec{\tau}\psi(x) \end{aligned} \tag{2.13}$$

and the evolution of the nucleon field is dictated by the equation

$$\left[\gamma^\mu (i\partial_\mu - g_\omega \omega_\mu(x) - \frac{1}{2} g_\rho \vec{\tau}\cdot\vec{\rho}_\mu(x)) - (m_N - g_\sigma \sigma(x))\right]\psi(x) = 0. \tag{2.14}$$

The above non-homogeneous coupled equations are fully relativistic and Lorentz covariant. However, their solution involves prohibitive difficulties, that can not be circumvented using approximations based on pertubation theory due to the high values of the coupling constants in the equations (2.12)-(2.14).
The scheme used to solve the above equations is the *mean field approximation*, that essentialy amounts to substituting the $\sigma(x)$, $\omega(x)$ and $\rho(x)$ quantum operators with the corresponding vacuum expectation value

$$\begin{aligned} \sigma(x) &\to \langle \sigma(x) \rangle = \langle 0|\sigma(x)|0\rangle, \\ \omega_\mu(x) &\to \langle \omega_\mu(x) \rangle = \langle 0|\omega_\mu(x)|0\rangle, \\ \rho_\mu(x) &\to \langle \rho_\mu(x) \rangle = \langle 0|\rho_\mu(x)|0\rangle. \end{aligned} \tag{2.15}$$

The mean field approximation is fully valid only when the baryon density n_B tends to infinity and the source terms of the equations of motion become so large that the quantum fluctuations of the mesonic fields are negligible. The extent to which the central density of neutron stars justifies its use depends on many factors, the most important of which is the mass of the star itself. Treating bosonic fields as classical objects, therefore, provides on the one hand a nonperturbative solution of the Eq.(2.14) but on the other hand it is only acceptable under certain conditions that are not always verified.
The use of this scheme is the reason for the absence of the nucleon-pion coupling in the interaction lagrangian. The pion field π, being at negative parity, has expactation value $\langle \pi(x) \rangle = 0$ for the invariance of the vacuum state under spatial inversion.
In uniform nuclear matter the baryon and scalar densities, $n_B = n_p + n_n = \langle \psi^\dagger \psi \rangle$ and $n_s = \langle \overline{\psi}\psi \rangle$, as well as isospin density, $\overline{\psi}(x)\gamma^0\tau_3\psi(x) = n_p - n_n$, and the current $j^\mu = \langle \overline{\psi}\gamma^\mu\psi \rangle$, are constants, independent of x. In addition, rotation invariance implies $\langle \overline{\psi}\gamma^i\psi \rangle = 0$ (i=1, 2, 3). Consequently, the mean values of the meson fields satisfy the relations

$$\begin{aligned} m_\sigma^2 \langle \sigma \rangle &= g_\sigma \langle \overline{\psi}\psi \rangle - \frac{g_\sigma^3}{G_3}\langle \sigma \rangle^2 - \frac{g_\sigma^4}{G_4}\langle \sigma \rangle^3 \\ &= g_\sigma n_s - \frac{g_\sigma^3}{G_3}\langle \sigma \rangle^2 - \frac{g_\sigma^4}{G_4}\langle \sigma \rangle^3 \end{aligned} \tag{2.16}$$

$$m_\omega^2\langle\omega^0\rangle = g_\omega\langle\overline{\psi}\gamma^0\psi\rangle = g_\omega n_B = g_\omega(n_p + n_n) \tag{2.17}$$

$$m_\rho^2\langle\rho^{03}\rangle = \frac{1}{2}g_\rho\langle\overline{\psi}\gamma^0\tau^3\psi\rangle = \frac{1}{2}g_\rho(n_p - n_n). \tag{2.18}$$

The terms of the equations of motion containing the derivatives cancel out due to the uniformity and staticity of the β-stable matter, the mean values of the spatial components of the fields $\omega(x)$ and $\rho(x)$ do not contribute for the rotation invariance of the vacuum state, and the action of the Pauli's matrices τ_1 and τ_2 on the isospinor $\psi(x)$, which does not mix the isospin quantum number, do not give projection on the adjoint $\overline{\psi}(x)$.
Instead of recalling the mean meson values, we retain their old names, but now without indicating an x dependence. The nucleon equation of motion reads

$$\left[\left(i\partial\!\!\!/ - g_\omega\gamma_\mu\omega^\mu - \frac{1}{2}g_\rho\gamma_\mu\tau^3\rho^{\mu 3}\right) - (m_N - g_\sigma\sigma)\right]\psi = 0, \tag{2.19}$$

that is a linear equation that can be exactly solved.
Because in the mean field approximation of uniform static matter, the nucleon fields satisfy an equation with no x-dependent terms, these fields are momentum eigenstates for the two isospin components which write as

$$\psi(x) = \psi^i(k)e^{-ik^\mu x_\mu} = \psi^i(k)e^{-i(k_0 t - \mathbf{k}\cdot\mathbf{x})}, \tag{2.20}$$

where $i = p, n$ and the four-spinors $\psi^i(k)$ being solutions of

$$\left[\gamma_\mu\left(k^\mu - g_\omega\omega^\mu \mp \frac{1}{2}g_\rho\rho^{\mu 3}\right) - (m_N - g_\sigma\sigma)\right]\psi^i(k) = 0 \tag{2.21}$$

where the minus sign is relative to protons, while the plus to neutrons.
The above equation can be recast in a form reminiscent of the Dirac equation for a non interacting nucleon. Defining

$$K^\mu = k^\mu - g_\omega\omega^\mu \mp \frac{1}{2}g_\rho\rho^{\mu 3} \tag{2.22}$$

$$m^* = m_N - g_\sigma\sigma \tag{2.23}$$

we obtain

$$\left(\gamma_\mu K^\mu - m^*\right)\psi^i(K) = 0. \tag{2.24}$$

The m^* is the effective mass. It is typical of the theories with scalar mesons that the fermion mass is altered in this above way. Note that the scalar field acts to reduce the effective nucleon mass.
The corresponding energy eigenvalues can be easily obtained using

$$\begin{aligned}\left(K\!\!\!/ + m^*\right)\left(K\!\!\!/ - m^*\right) &= K\!\!\!/\,K\!\!\!/ - m^{*2} = K^\mu K^\nu\gamma_\mu\gamma_\nu - m^{*2} \\ &= K^\mu K^\nu\frac{\gamma_\mu\gamma_\nu + \gamma_\nu\gamma_\mu}{2} - m^{*2} \\ &= K^\mu K_\mu - m^{*2}.\end{aligned} \tag{2.25}$$

Substitution in Eq.(2.24) yields

$$\begin{aligned}\Big(K^\mu K_\mu - m^{*2}\Big)\psi^i(K) = 0 \\ \Rightarrow \Big(K^\mu K_\mu - m^{*2}\Big) = 0.\end{aligned} \tag{2.26}$$

We obtain

$$K^0 = \sqrt{\mathbf{K}^2 + m^{*2}} \tag{2.27}$$

and denoting the time component of the four-vector $k \equiv (k^0, \mathbf{k})$ by

$$e(\mathbf{k}) = k^0(\mathbf{k}) \equiv K^0 + g_\omega \omega^0 \pm \frac{1}{2} g_\rho \rho^{03}. \tag{2.28}$$

Hence the nucleon eigenvalues of 3-momentum $\mathbf{k}$ for particle and antiparticle are

$$\begin{aligned}e(\mathbf{k}) &= g_\omega \omega^0 \pm \frac{1}{2} g_\rho \rho^{03} + E(\mathbf{k}), \\ \overline{e}(\mathbf{k}) &= g_\omega \omega^0 \pm \frac{1}{2} g_\rho \rho^{03} - E(\mathbf{k})\end{aligned} \tag{2.29}$$

with

$$E(\mathbf{k}) \equiv K^0 = \sqrt{\left(\mathbf{k} - g_\omega \boldsymbol{\omega} \mp \frac{1}{2} g_\rho \boldsymbol{\rho}^3\right)^2 + m^{*2}}. \tag{2.30}$$

It should be noted that, since the zero temperature approximation is entirely justified for nuclear matter in the core of neutron stars, negative energy solutions, which represent antineutrons and antiprotons, do not participate in the evolution of the medium. They derive from the creation of particle-antiparticle pairs, made possible only through termal excitations.

The above equations give the Dirac momentum eigenvalues expressed in terms of the mean values of the meson fields, which are in turn defined in terms of the ground state expectation values of the nucleon densities and current, according to Eqs. (2.16)-(2.18).

The ground state expectation value of an operator $\overline{\psi}\Gamma\psi$ can be evaluated exploiting the fact that each nucleon state is specified by its momentum, k, and intrinsic spin projection. Denoting the average of $\overline{\psi}\Gamma\psi$ in a single particle state by $\langle\overline{\psi}\Gamma\psi\rangle_{\mathbf{k}\alpha}$, where the index α labels the spin state, we can write the ground state expectation value of an operator as

$$\langle\overline{\psi}\Gamma\psi\rangle = \sum_\alpha \int \frac{d^3k}{(2\pi)^3} \langle\overline{\psi}\Gamma\psi\rangle_{\mathbf{k}\alpha} \Theta(e_F - e(\mathbf{k})) \tag{2.31}$$

where the Θ-function restricts the momentum integration to the region corresponding to energies lower than the Fermi energy e_F.

Using the Dirac equation (2.21) and isolating k^0, we can find the *Dirac Hamiltonian*:

$$H_D = \gamma_0 \Big[\boldsymbol{\gamma} \cdot \mathbf{k} + g_\omega \gamma_\mu \omega^\mu \pm \frac{1}{2} g_\rho \gamma_\mu \rho^{\mu 3} + m^*\Big]. \tag{2.32}$$

Now, take the expectation in a single-nucleon momentum state as defined above:

$$\langle H_D\rangle_{\mathbf{k}\alpha} = \langle\psi^\dagger H_D \psi\rangle_{\mathbf{k}\alpha} = g_\omega \omega^0 \pm \frac{1}{2} g_\rho \rho^{03} + E(\mathbf{k}). \tag{2.33}$$

It should be noted that the right side is independent of the spin projection label α, i.e. the momentum states are degenerate.
The ground state expectation value of the baryon density can be readily evaluated from Eqs. (2.32) and (2.33) noting that

$$\begin{aligned}\frac{\partial}{\partial\omega^0}\langle\psi^\dagger H_D\psi\rangle_{\mathbf{k}\alpha} &= \frac{\partial}{\partial\omega^0}\left(g_\omega\omega^0 \pm \frac{1}{2}g_\rho\rho^{03} + E(\mathbf{k})\right) = g_\omega \\ &= \langle\psi^\dagger\frac{\partial H_D}{\partial\omega^0}\psi\rangle_{\mathbf{k}\alpha} = g_\omega\langle\psi^\dagger\psi\rangle_{\mathbf{k}\alpha}\end{aligned} \tag{2.34}$$

implying

$$\langle\psi^\dagger\psi\rangle_{\mathbf{k}\alpha} = 1. \tag{2.35}$$

Then from (2.31) we have the baryon density, but since the system of interest is isospin asymmetric, it is convenient to separate the densities of proton and neutron

$$n_i = \langle\psi^\dagger\psi\rangle = 2\int\frac{d^3k}{(2\pi)^3}\Theta(e_{Fi} - e(\mathbf{k})), \tag{2.36}$$

where 2 indicates the spin degeneracy of the momentum egeinstate, $i = p, n$ and e_{Fi} is the Fermi energy of the relative nucleon.
The same procedure can be applied to compute the ground state expectation value $\langle\overline{\psi}\gamma^i\psi\rangle$ $i = 1, 2, 3$. Taking the derivative with respect to k_i we find

$$\begin{aligned}\frac{\partial}{\partial k_i}\langle\psi^\dagger H_D\psi\rangle_{\mathbf{k}\alpha} &= \frac{\partial}{\partial k_i}\left(g_\omega\omega^0 \pm \frac{1}{2}g_\rho\rho^{03} + E(\mathbf{k})\right) = \frac{\partial E(\mathbf{k})}{\partial k_i} \\ &= \langle\psi^\dagger\frac{\partial H_D}{\partial k_i}\psi\rangle_{\mathbf{k}\alpha} = g_\omega\langle\psi^\dagger\gamma^0\gamma^i\psi\rangle_{\mathbf{k}\alpha} = \langle\overline{\psi}\gamma^i\psi\rangle_{\mathbf{k}\alpha}\end{aligned} \tag{2.37}$$

leading to

$$\begin{aligned}\langle\overline{\psi}\gamma^i\psi\rangle &= 2\int\frac{d^3k}{(2\pi)^3}\left(\frac{\partial E(\mathbf{k})}{\partial k_i}\right)\Theta(e_F - e(\mathbf{k})) \\ &= \frac{2}{(2\pi)^3}\int\sum_{j\neq i}dk_j\int dE_{\mathbf{k}}\Theta(e_F - e(\mathbf{k})) = 0.\end{aligned} \tag{2.38}$$

The integral is over the occupied momentum states, i.e. over some volume in the momentum space. The integral above vanishes because $E(\mathbf{k})$ equals the constant $e_F - g_\omega\omega^0 \mp \frac{1}{2}g_\rho\rho^{03}$ everywhere on the boundary of the surface of the integration region. Thus, the integral over dE is the difference of two equal numbers.
The vanishing of the baryon current had been anticipated noting that in uniform matter the mean values of the space components of the vector fields vanish, i.e. that $\langle\omega^i\rangle = \langle\rho^i\rangle = 0$. Consequently, the energy eigenvalues depend upon the magnitude of the nucleon momentum only, according to

$$e(\mathbf{k}) = g_\omega\omega^0 \pm \frac{1}{2}g_\rho\rho^{03} + \sqrt{|\mathbf{k}|^2 + m^{*2}}, \tag{2.39}$$

and the occupied region of momentum space is a sphere. The baryon density (2.36) takes the familiar form

$$n_i = \frac{2}{(2\pi)^3}\int_0^{k_{Fi}}d^3k = \frac{k_{F_i}^3}{3\pi^2}, \tag{2.40}$$

k_{F_i} is the Fermi momentum of the corresponding nucleon, that is related to Fermi energy e_{Fi} through the Eq. (2.39)

$$e_{Fi} = g_\omega \omega^0 \pm \frac{1}{2} g_\rho \rho^{03} + \sqrt{|\mathbf{k}_{Fi}|^2 + m^{*2}}, \tag{2.41}$$

where for $i = p$ the sign of the second term is plus, for $i = n$ minus.
Finally, the scalar density $n_s = \langle \overline{\psi}\psi \rangle$ can be evaluated taking the derivative of (2.33) with respect to m:

$$\frac{\partial}{\partial m}\langle \psi^\dagger H_D \psi \rangle_{\mathbf{k}\alpha} = \frac{\partial E(\mathbf{k})}{\partial m} = \langle \psi^\dagger \frac{\partial H_D}{\partial m} \psi \rangle_{\mathbf{k}\alpha} = \langle \psi^\dagger \gamma^0 \psi \rangle_{\mathbf{k}\alpha} = \langle \overline{\psi}\psi \rangle_{\mathbf{k}\alpha}, \tag{2.42}$$

yielding

$$\langle \overline{\psi}\psi \rangle_{\mathbf{k}\alpha} = \frac{m^*}{\sqrt{|\mathbf{k}|^2 + m^{*2}}}, \tag{2.43}$$

and

$$\langle \overline{\psi}\psi \rangle = \frac{1}{\pi^2} \int_0^{k_F} k^2 dk \frac{m^*}{\sqrt{|\mathbf{k}|^2 + m^{*2}}}. \tag{2.44}$$

Collecting together the results of Eqs. (2.36), (2.38) and (2.44) we can rewrite the equations of motion (2.16)-(2.18) in the form:

$$m_\sigma^2 \sigma = g_\sigma \frac{1}{\pi^2} \sum_{i=p,n} \int_0^{k_{F_i}} k^2 dk \frac{m^*}{\sqrt{|\mathbf{k}|^2 + m^{*2}}} - \frac{g_\sigma^3}{G_3}\sigma^2 - \frac{g_\sigma^4}{G_4}\sigma^3 \tag{2.45}$$

$$m_\omega^2 \omega^0 = g_\omega \frac{1}{3\pi^2}(k_{F_p}^3 + k_{F_n}^3) \tag{2.46}$$

$$m_\rho^2 \rho^{03} = \frac{1}{2} g_\rho \frac{1}{3\pi^2}(k_{F_p}^3 - k_{F_n}^3). \tag{2.47}$$

The last two are trivial, but the first expresses a self-consistency reuqirement on the mean value of the scalar field, whose value has to satisfy a trascendental equation.

2.2.2 Equation of state

To compute the equation of state, i.e the relation between pressure, or energy, and density of matter, in quantum field theory we start from the energy-momentum tensor, that for a generic Lagrangian $\mathcal{L} = \mathcal{L}(\Phi, \partial_\mu \Phi)$ can be written

$$T^{\mu\nu} = \frac{\partial \mathcal{L}}{\partial(\partial_\mu \Phi)} \partial^\nu \Phi - \eta^{\mu\nu} \mathcal{L}, \tag{2.48}$$

where $\eta^{\mu\nu} = diag(1, -1, -1, -1)$ is the Minkowski tensor.[1].
In an uniform system the expectation value of $T^{\mu\nu}$ is directly related to the energy density, ϵ, and pressure, P, through

$$\langle T_{\mu\nu} \rangle = u_\mu u_\nu (\epsilon + P) - \eta_{\mu\nu} P, \tag{2.49}$$

[1]This tensor will be discussed and generalized in Chapter 4.

where u denotes the four velocity of the system, satisfying $u_\mu u^\mu = 1$. It follows that in the reference frame in which matter is at rest $\langle T_{\mu\nu}\rangle$ is diagonal and

$$\epsilon = \langle T_{00}\rangle = \langle \overline{\psi}\gamma_0 k_0 \psi\rangle - \langle \mathcal{L}\rangle, \tag{2.50}$$

$$P = \frac{1}{3}\langle T_{ii}\rangle = \frac{1}{3}\langle \overline{\psi}\gamma_i k_i \psi\rangle + \langle \mathcal{L}\rangle. \tag{2.51}$$

Within the mean field approximation, the two above equations reduce to

$$\begin{aligned}
\epsilon &= \langle \overline{\psi}\gamma_0 k_0 \psi\rangle + \tfrac{1}{2}m_\sigma^2\sigma^2 - \tfrac{1}{2}m_\omega^2\omega^2 - \tfrac{1}{2}m_\rho^2\rho^2 + \tfrac{1}{3}\tfrac{g_\sigma^3}{G_3}\sigma^3 + \tfrac{1}{4}\tfrac{g_\sigma^4}{G_4}\sigma^4 \\
&= \langle \overline{\psi}\gamma_0 k_0 \psi\rangle - \tfrac{1}{2}\tfrac{g_\omega^2}{m_\omega^2}\langle \overline{\psi}\gamma_0\psi\rangle^2 - \tfrac{1}{8}\tfrac{g_\rho^2}{m_\rho^2}\langle \overline{\psi}\gamma_0\tau_3\psi\rangle^2 + \\
&+ \tfrac{1}{2}m_\sigma^2\sigma^2 + \tfrac{1}{3}\tfrac{g_\sigma^3}{G_3}\sigma^3 + \tfrac{1}{4}\tfrac{g_\sigma^4}{G_4}\sigma^4 \,.
\end{aligned} \tag{2.52}$$

$$\begin{aligned}
P &= \tfrac{1}{3}\langle \overline{\psi}\gamma_i k_i \psi\rangle - \tfrac{1}{2}m_\sigma^2\sigma^2 + \tfrac{1}{2}m_\omega^2\omega^2 + \tfrac{1}{2}m_\rho^2\rho^2 - \tfrac{1}{3}\tfrac{g_\sigma^3}{G_3}\sigma^3 - \tfrac{1}{4}\tfrac{g_\sigma^4}{G_4}\sigma^4 \\
&= \tfrac{1}{3}\langle \overline{\psi}\gamma_i k_i \psi\rangle + \tfrac{1}{2}\tfrac{g_\omega^2}{m_\omega^2}\langle \overline{\psi}\gamma_0\psi\rangle^2 + \tfrac{1}{8}\tfrac{g_\rho^2}{m_\rho^2}\langle \overline{\psi}\gamma_0\tau_3\psi\rangle^2 + \\
&- \tfrac{1}{2}m_\sigma^2\sigma^2 - \tfrac{1}{3}\tfrac{g_\sigma^3}{G_3}\sigma^3 - \tfrac{1}{4}\tfrac{g_\sigma^4}{G_4}\sigma^4 \,.
\end{aligned} \tag{2.53}$$

Togheter they are referred to as the equation of state.
There are still two terms to calculate. Using Eqs. (2.33), (2.39) and (2.46)-(2.47)

$$\begin{aligned}
\langle \overline{\psi}\gamma_0 k_0 \psi\rangle &= \frac{1}{\pi^2}\int_0^{k_{Fp}} dk k^2 \left[g_\omega\omega^0 + \frac{1}{2}g_\rho\rho^{03} + \sqrt{k^2+m^{*2}}\right] + \\
&+ \frac{1}{\pi^2}\int_0^{k_{Fn}} dk k^2 \left[g_\omega\omega^0 - \frac{1}{2}g_\rho\rho^{03} + \sqrt{k^2+m^{*2}}\right] \\
&= m_\omega^2\omega_0^2 + m_\rho^2\rho_{03}^2 + \\
&+ \frac{1}{\pi^2}\left[\int_0^{k_{Fp}} dk k^2\sqrt{k^2+m^{*2}} + \int_0^{k_{Fn}} dk k^2\sqrt{k^2+m^{*2}}\right],
\end{aligned} \tag{2.54}$$

and considering Eq. (2.38)

$$\langle \overline{\psi}\gamma_i k_i \psi\rangle = \langle \overline{\psi}(\boldsymbol{\gamma}\cdot\mathbf{k})\psi\rangle = \frac{1}{\pi^2}\left[\int_0^{k_{Fp}} dk \frac{k^4}{\sqrt{k^2+m^{*2}}} + \int_0^{k_{Fn}} dk \frac{k^4}{\sqrt{k^2+m^{*2}}}\right]. \tag{2.55}$$

Therefore, the equations become

$$\begin{aligned}
\epsilon &= \tfrac{1}{2}m_\sigma^2\sigma^2 + \tfrac{1}{2}m_\omega^2\omega_0^2 + \tfrac{1}{2}m_\rho^2\rho_{03}^2 + \tfrac{1}{3}\tfrac{g_\sigma^3}{G_3}\sigma^3 + \tfrac{1}{4}\tfrac{g_\sigma^4}{G_4}\sigma^4 + \\
&+ \tfrac{1}{\pi^2}\textstyle\sum_{i=p,n}\displaystyle\int_0^{k_{F_i}} k^2 dk \sqrt{|\mathbf{k}|^2 + m^{*2}},
\end{aligned} \tag{2.56}$$

and

$$\begin{aligned}
P &= -\tfrac{1}{2}m_\sigma^2\sigma^2 + \tfrac{1}{2}m_\omega^2\omega_0^2 + \tfrac{1}{2}m_\rho^2\rho_{03}^2 - \tfrac{1}{3}\tfrac{g_\sigma^3}{G_3}\sigma^3 - \tfrac{1}{4}\tfrac{g_\sigma^4}{G_4}\sigma^4 + \\
&+ \tfrac{1}{3\pi^2}\textstyle\sum_{i=p,n}\displaystyle\int_0^{k_{F_i}} dk \frac{k^4}{\sqrt{k^2+m^{*2}}}
\end{aligned} \tag{2.57}$$

The terms of the first row of the two equations derive from the dynamics of mesonic fields while the final integrals contain information on the kinematics of relativistic gases of baryons with effective masses m^*.
The expression of the effective mass, that is one of the main properties of the nuclear matter as discussed in Section (2.1), can be evaluated by rearranging, and making integrals, the Eqs. (2.23) and (2.45). It reads:

$$\begin{aligned} m^* &= m_N + \frac{g_\sigma^4}{m_\sigma^2}\frac{\sigma^2}{G_3} + \frac{g_\sigma^5}{m_\sigma^2}\frac{\sigma^3}{G_4} + \\ &- \frac{g_\sigma^2}{m_\sigma^2}\frac{m^*}{\pi^2}\sum_{i=p,n}\left[k_{Fi}\sqrt{k_{Fi}^2+m^{*2}} - m^{*2}\ln\left(\frac{k_{Fi}+\sqrt{k_{Fi}^2+m^{*2}}}{m^*}\right)\right]. \end{aligned} \tag{2.58}$$

Equations (2.56)-(2.58) yield energy density and pressure of nuclear matter as a function of the baryon number density $n_B = n_p + n_n$, recalling $k_F = (3\pi n)^{1/3}$ for the two nucleons.
At saturation point of nuclear matter only the neutron and proton states are populated. They are are equally coupled to the meson fields. It is possible to see from equations (2.45)-(2.47) that the field variables are $g_\sigma\sigma$, $g_\omega\omega^0$ and $g_\rho\rho^{03}$ and that the solution depends on coupling constants and masses only through the ratio $(g_\sigma/m_\sigma)^2$, $(g_\omega/m_\omega)^2$ and $(g_\rho/m_\rho)^2$.
The bulk properties of nuclear matter discussed at the beginning of the chapter, Section (2.1), can be used to determine the five parameters of the Lagrangian, i.e. the three ratios which have just been mentioned and in addition the constants, G_3 and G_4, of the scalar self-interaction terms. Usually the latter two constants are redefined as $b \equiv \frac{1}{m_N G_3}$ and $c \equiv \frac{1}{G_4}$, that are dimensionless quantities.
The scenario changes completely with the presence of hyperons, that by appearing at much higher densities do not populate the fundamental states and consequently there is no longer background informations on the properties of hadronic matter at saturation. This makes it much more difficult to determine constraints on hyperon couplings and control the properties of the hadronic stars.
In the following chapter, σ-ω-ρ model will be generalized to the strange baryon matter.

Chapter 3

Strange baryon matter

In addition to the similarities that were discussed in the first chapter between the properties of the interior of nuclei inner and the matter of neutron stars, there are also relevant differences mainly due to two reasons: charge neutrality and generalized beta equilibrium without conservation of strangeness.
The reason being of neutron stars is to be neutral [12]. The neutron stars are held together by the gravitational attraction and take into account the balance between the repulsive Coulomb force acting on a charged particle of the same sign as the net charge of the star (Z_{net}) and the gravitational force. Considering the particle to be located at the surface of the star, it will be expelled out unless the gravitational force overcomes the Coulomb force. For the proton, the corresponding limit on the net positive charge of the star is $Z_{net}/A \sim 10^{-36}$ [4]. For the electron, this limit would be reduced by the factor m_e/m_p. Hence, the net charge per charged particle is practically zero. This result leads to the conclusion that a neutron star is electrically neutral. This fact is achievied even if the number of protons Z is not zero because the proton charge can be neutralized by leptons or negatively charged hyperons and so $Z < A/2$ and generally much smaller. Instead, in nuclei is true that $Z \approx A/2$ since they are bound by the isospin symmetric nuclear force and not by gravity. Thus, nuclei tend to be symmetric in isospin whereas neutron stars are very asimmetric.
In order to explain the second reason, we have to consider the weak interaction timescale, that is $\tau_{weak} \sim 10^{-10}$ seconds. Since the high density of neutron stars and that the baryons obey the Pauli principle, for nucleons at the top of the Fermi sea it becomes energetically favorable to convert to other baryons, including hyperons, so as to lower Fermi energies. The reactions that occur, as we will see in the next section, can do so both on timescale of strong and weak interactions. In the first case the strangeness is conserved, in the second no. Thus the neutron stars have net strangeness. This is a significant difference compared to nuclei, in which strangeness would not be conserved but it is not energetically favorable the hyperon appearence in the ground state because their masses exceed the nucleon mass by more than the Fermi energy (∼30 MeV) of the nucleons. However nuclear reactions are so fast ($\sim 10^{-22}$ s) that strangeness is conserved on their timescale and so the nuclear matter has zero net strangeness.
Neither lepton number, even if the timescale is longer (of the order of tens of seconds),

is conserved because of neutrino leakage out. Indeed, at the typical temperature of neutron star interior the neutrino mean free path in nuclear matter is much larger than the typical radius of neutron star, $R \sim (10 - 15)$ km. Therefore, neutron stars are transparent to neutrinos.
In this chapter we introduce the generalization of relativistic, mean field theory to include higher mass baryons tha was first implemented by Garpman, Glendenning and Karant [13]. The most important baryons are the remaining members of the lowest baryon octet, the hyperons Λ, Σ, Ξ. Their properties, together with those of nucleons, are summarised in Table 3.1.

	M [MeV]	J	I_3	q	s
p	938.3	1/2	1/2	+1	0
n	939.6	1/2	-1/2	0	0
Λ^0	1115.7	1/2	0	0	-1
Σ^-	1197.4	1/2	-1	-1	-1
Σ^0	1192.6	1/2	0	0	-1
Σ^+	1189.4	1/2	+1	+1	-1
Ξ^0	1314.8	1/2	1/2	0	-2
Ξ^-	1321.3	1/2	-1/2	-1	-2

Table 3.1. Properties of nucleons and strange baryons: mass M, spin J, isospin projection I_3, charge q and strangeness s.

Note that since of the charge neutrality of neutron stars and the interaction with the ρ meson, it is essential to distinguish the various isospin and charge states. Therefore, the case of nucleons with different isospin projection, which we discussed earlier, is a special case and readily generalized.
First, however, we need to discuss carefully the equilibrium conditions which determine the appeareance and abundance of hyperon species in neutron star cores.

3.0.1 Equilibrium conditions for strange baryon stars

During the evolution of a star several reactions can occur and a cold neutron star is a possible ground state configuration. Moreover, there are quantum numbers that are conserved absolutely on a long timescale in comparision to the lifetime of the star and others that are violated by weak and electromagnetic interactions on a short timescale. The ground state can be seen as a problem of chemical equilibrium subject only to the constraints of baryon and electric-charge number, while the strangeness quantum number, for instance, provides no constraints on the star evolution.
When the Fermi momentum of nucleons becomes sufficiently high, strong reactions as

$$N + N \rightarrow N + \Lambda + K \tag{3.1}$$

are possible. The produced kaon decays on a time scale $\sim 10^{-10}$ s in processes like

$$\begin{aligned} K^0 &\to 2\gamma, \\ K^- &\to \mu^- + \overline{\nu}, \\ \mu^- + K^+ &\to \mu^- + \mu^+ + \nu \to 2\gamma + \nu. \end{aligned} \tag{3.2}$$

The temperature of the star is lowered through the neutrino loss and, strong interactions such as (3.1) no longer take place because the energy required to create the kaon is not available. Despite this the strangeness continues to grow through direct weak interaction processes such as

$$p + e^- \to \Lambda^0 + \nu_e \tag{3.3}$$

$$p + e^- \to \Sigma^0 + \nu_e \tag{3.4}$$

$$n + e^- \to \Sigma^- + \nu_e. \tag{3.5}$$

Moreover, the leakage of photons in addition to that of neutrinos significantly lowers the star's energy and, consequently, the Λ becomes Pauli blocked, the reactions (3.1) and (3.3)-(3.5) become irreversible, and a net strangeness is evolved.
This type of processes go on until the star reaches its ground state, i.e. the degenerate state in which the lepton and baryon populations are distribuited among the various species under zero net charge constraint. All neutrinos and photons have leaked out.
Let us now discuss directly the problem of the chemical equilibrium of the ground state. Considering a system, that is a generalization of equations (3.3)-(3.5), consisting of B baryonic species $b_1 ... b_B$ and L leptonic species $\ell_1 ... \ell_L$, in equilibrium with respect to the weak interaction processes

$$b_i \to b_j + \ell_k + \overline{\nu}_\ell, \tag{3.6}$$

$$b_j + \ell_k \to b_i + \nu_\ell, \tag{3.7}$$

with $i, j = 1...B$ and $k = 1...L$. The ground state of system, specified by the densities of the constituent particles, n_{b_i} and n_{ℓ_i}, is determined by minimization of energy density with the constraints dictated from conservation of the baryon density, n_B, and charge neutrality, implying

$$\sum_{i=1}^{B} n_{b_i} = n_B, \tag{3.8}$$

$$\sum_{i=1}^{B} q_{b_i} n_{b_i} + \sum_{i=1}^{L} q_{\ell_i} n_{\ell_i} = 0, \tag{3.9}$$

where q_{b_i} and q_{ℓ_i} denote the electric charge of the i-th baryonic and leptonic species, respectively.
Minimization of energy density ϵ with respect to the densities n_{b_i} and n_{ℓ_i} with the above contraints results in $L + B$ equations involving the chemical potentials of the constituents

$$\mu_{b_i} = \frac{\partial \epsilon}{\partial n_{b_i}}, \qquad \mu_{\ell_i} = \frac{\partial \epsilon}{\partial n_{\ell_i}}. \tag{3.10}$$

There are as many independent chemical potentials as there are conserved quantities. All other chemical potentials can be expressed in terms of the independent ones. For example, at densities in the vicinity of nuclear matter density, charge-neutral matter is almost entirely composed of neutrons, but must have a small admixture of protons with equal number of electrons for establish equilibrium with respect to $n \leftrightarrow p + e^- + \overline{\nu}_e$. For a cold star, equilibrium is reached when the Fermions occupy their lower energy states up to energies that satisfy the balance

$$\mu_p = \mu_n + \mu_e, \tag{3.11}$$

considering that neutrino chemical potentials are zero in the evolved star. This is the case of beta equilibrium, which was anticipated in Section 1.1.3. The above equation is explicitly derived through the minimalization of energy density in Appendix A. In the following when the matter will be defined as β-stable, we will mean a general β equilibrium that refers to equilibrium with respect to all processes that lead to the transmutation of baryons by strong and weak interactions until to the lowest energy state that is consistent with charge neutrality. Therefore, possible meson condensation and a deconfined quark phase are ignored.
As the baryon density increases, so does that of electrons and protons. Thus, μ_e may attain the value of muon mass, in which case it also will be populated. The equilibrium is assured when

$$\mu_\mu = \mu_e. \tag{3.12}$$

The electromagnetic and weak decays (3.2) with the vanishing populations of photons and neutrinos imply that

$$\mu_{K^0} = 0, \qquad \mu_{K^-} = \mu_e, \qquad \mu_{K^+} = -\mu_e. \tag{3.13}$$

Moreover, equilibrium with respect to (3.1) coupled with the decay of the K^0 into gamma rays yields

$$\mu_\Lambda = \mu_n. \tag{3.14}$$

The chemical potentials of the other hyperons can be inferred likewise. For instance, the process (3.5) tell us that

$$\mu_{\Sigma^-} = \mu_n + \mu_e. \tag{3.15}$$

Considering the several chemical potential relations obtained, it is clear that there are only two independent chemical potentials, i.e. μ_n and μ_e. Therefore, in general, the chemical potential of any particle is a linear combination of these two, weighted by the baryon (b) and electric (q) charge carried by the particle,

$$\begin{aligned} \mu_i &= b\mu_n - q\mu_e \\ &\Rightarrow \mu_B = \mu_n - q_B\mu_e. \end{aligned} \tag{3.16}$$

The implication indicates the form of the equation in the specific case of baryons. Treating all constituents as non interacting particles, one finds that Σ^- and Λ^0 appear at densities $\sim 4n_0$ and $\sim 8n_0$, respectively, n_0 being the equilibrium density of isospin-symmetric nuclear matter.
Note that the density at which the production of a strange hadron is expected to

occur do not depend on its mass only. Let us consider the Λ^0 and Σ^- hyperons, whose appearance becomes energetically favoured as soon as the threshold conditions

$$\mu_n + \mu_e = M_{\Sigma^-}, \qquad \mu_n = M_{\Lambda^0}, \tag{3.17}$$

are fulfilled. From the above relations it follows that, in spite of the larger mass, the threshold density of Σ^- production is in fact lower than that of Λ^0 production if the electron chemical potential is such that

$$\mu_e > M_{\Sigma^-} - M_{\Lambda^0} \approx 80\,\mathrm{MeV}. \tag{3.18}$$

The corresponding electron density can be easily obtained, and the threshold condition takes the form

$$\mu_e = \sqrt{k_{Fe}^2 + m_e^2} \approx k_{Fe} = (3\pi^2 n_e)^{1/3} > 80\,\mathrm{MeV}, \tag{3.19}$$

implying

$$n_e \gtrsim 2 \times 10^{-3}\,\mathrm{fm}^{-3}. \tag{3.20}$$

Under the reasonable assumption that the electron density be of the order of one percent of the baryon density, the above estimate corresponds to $n_B > 0.2\,\mathrm{fm}^{-3} \gtrsim \mathrm{n}_0$, a density that is certainly reached in compact stars.

Considering interactions, the critical density for the onset of a species considerably change. The results of theoretical calculations suggest that hyperons appear at densities $n \gtrsim 2n_0$ and that by $n \approx 3n_0$ they sustain a significant fraction of the total baryon population. At even larger density, $n > 4n_0$, a new transition, to a phase in which quarks are no longer clustered into hadrons is eventually expected to take place.

Thus, the first hyperon species that appears is the Σ^-, closely followed by the Λ. However, the formation of Σ^- hyperons is rapidly moderated by the isospin dependent forces that disfavor an excess of Σ^-'s over Σ^+'s, and also joint excess of Σ^-'s and neutrons, both of negative isospin projection. Therefore, the Σ^- density saturates earlier than Λ's, free of isospin-dependent forces, that continue to accumulate until short range repulsion forces also cause their saturation. Other hyperon species like Ξ's follow at higher densities.

However, the composition of neutron star matter is largely controlled by the hyperon-nucleon interactions. If any reaction is assumed to be highly repulsive, the formation of some species may become suppressed. For instance, considering a strongly repulsion between Σ hyperons and nucleons, as it has been suggested on the results of many works about Σ^- atoms [14], Σ's do not form in neutron star matter. Consequently, Λ formation begins at slighlty lower densities than when Σ's are present. As a result, Ξ also appears at lower densities. The overall strangeness fraction continues to remain similar to the case when there is Σ^- population.

Finally it should be noted that hyperon appeareance provides an immediate deleptonization of the matter, that is particular strong when Ξ formation occurs. In this latter case the muon population is entirely extinguished, and the electron fraction drops below 1%, whereas it exceeds 10% in the nuclear matter case. Leptons survive in nuclear matter basically to maintain charge neutrality with protons, but they are very expensive in terms of pressure and energy density. Hyperons are an option for

lowering the neutron excess without a lepton formation, and the negatively charged hyperons allow charge neutrality to be maintained within the baryon population. An example of the estimates for hyperon formation in neutron star matter, as found in many works, is displayed in Fig. 3.1. It should be remarked that the onset of the different species of hyperons may change depending on how the hadronic interactions of the theory used are modeled.

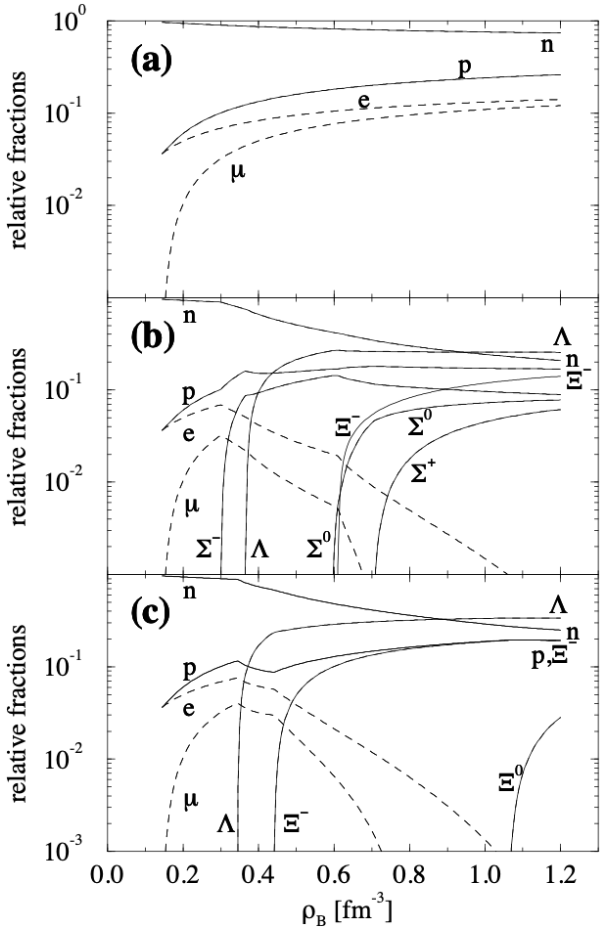

Figure 3.1. Relative fractions of the equilibrium composition of neutron star matter as a function of the baryon density, [14]: (a) nuclear matter witouth hyperons (b) matter with nucleons and all hyperons, considering the interaction of Σ hyperons and nucleons equal to the Λ-nucleons case, except for the isospin contribution (c) matter with nucleons, Λ and Ξ hyperons but no Σ's due to introduction of a strongly repulsive component in the potential of Σ hyperons in nuclear matter.

3.0.2 Strange generalization of σ-ω-ρ model

A suitable generalization of the Lagrangian (2.7) is

$$\begin{aligned}\mathcal{L} =& \sum_B \overline{\psi}_B(i\partial\!\!\!/ - m_B + g_{\sigma B}\sigma - g_{\omega B}\gamma_\mu\omega^\mu - \frac{1}{2}g_{\rho B}\gamma_\mu\boldsymbol{\tau}\cdot\boldsymbol{\rho}^\mu)\psi_B \\ &+ \frac{1}{2}(\partial_\mu\sigma\partial^\mu\sigma - m_\sigma^2\sigma^2) - \frac{1}{4}F_{\mu\nu}F^{\mu\nu} + \frac{1}{2}m_\omega^2\omega_{\mu\nu}\omega^{\mu\nu} \\ &- \frac{1}{4}B_{\mu\nu}B^{\mu\nu} + \frac{1}{2}m_\rho^2\rho_{\mu\nu}\rho^{\mu\nu} - \frac{1}{3}bm_N(g_\sigma\sigma)^3 - \frac{1}{4}c(g_\sigma\sigma)^4 \\ &+ \sum_{\ell=e^-,\mu^-} \overline{\psi}_\ell(i\partial\!\!\!/ - m_\ell)\psi_\ell.\end{aligned} \tag{3.21}$$

We use the notation b, c for the scalar self interaction terms as mentioned at the end of the previous chapter.
The spinor for the baryon species B, one of those listed in Table 3.1 or that Δ quartet, is denoted by ψ_B. In this work we use the assumption that Δ isobars do not appear in neutron star matter. The reason of this choice is that Δ would appear at densities much higher than the typical densities of the core of neutron stars due to a strong isovector repulsion, and so they are therefore irrelevant for astrophysics [12]. Morever, the free Lagrangians for the leptons, electrons and muons, are introduced to complete the scheme describing the baryon stars.
The Euler-Lagrange equations follow from the above Lagrangian. In the mean field approximation, the Dirac equations in uniform matter for each species B are

$$\left[\gamma_\mu\left(k^\mu - g_{\omega B}\omega^\mu - \frac{1}{2}g_{\rho B}\tau_3\rho^{\mu 3}\right) - (m_B - g_{\sigma B}\sigma)\right]\psi_B(k) = 0. \tag{3.22}$$

The eigenvalues of particle can be found as

$$e_B(\mathbf{k}) = g_{\omega B}\omega_0 + g_{\rho B}\rho_{03}I_{3B} + \sqrt{k^2 + (m_B - g_{\sigma B}\sigma)^2} \tag{3.23}$$

where I_{3B} is the isospin 3-component for baryon B. We have explicity used the fact, derived in Section 2.2.1, that only the isospin 3-component of the ρ field remains in the mean field approximation and that the Lorentz three-current part of the ω and ρ fields vanish in the static ground state of matter.
The meson fields equations in uniform static matter are

$$\begin{aligned}m_\sigma^2\sigma = \sum_B \frac{2J_B+1}{2\pi^2}g_{\sigma B}\int_0^{k_{F_B}} k^2dk\frac{m_B - g_{\sigma B}\sigma}{\sqrt{k^2 + (m_B - g_{\sigma B}\sigma)^2}} \\ - bm_N g_\sigma^3\sigma^2 - cg_\sigma^4\sigma^3\end{aligned} \tag{3.24}$$

$$\omega^0 = \sum_B \frac{g_{\omega B}}{m_\omega^2}(2J_B+1)\frac{k_{F_B}^3}{6\pi^2} \tag{3.25}$$

$$\rho^{03} = \sum_B \frac{g_{\rho B}}{m_\rho^2}I_{3B}(2J_B+1)\frac{k_{F_B}^3}{6\pi^2}, \tag{3.26}$$

using $g_i \equiv g_{iN}$ with $i = \sigma, \omega, \rho$ to denote the nucleon couplings while for the other baryons g_{iB}.

The energy density and pressure, including lepton contributions always evaluated using Eqs. (2.54) and (2.55), can be found and read

$$\begin{aligned}\epsilon &= \tfrac{1}{2}m_\sigma^2\sigma^2+\tfrac{1}{2}m_\omega^2\omega_0^2+\tfrac{1}{2}m_\rho^2\rho_{03}^2+\tfrac{1}{3}bm_N(g_\sigma\sigma)^3+\tfrac{1}{4}c(g_\sigma\sigma)^4+\\ &+ \textstyle\sum_B \frac{2J_B+1}{2\pi^2}\int_0^{k_{F_B}} k^2dk\sqrt{k^2+(m_B-g_{\sigma B}\sigma)^2}+\\ &+ \textstyle\sum_\ell \frac{1}{\pi^2}\int_0^{k_{F_\ell}} k^2dk\sqrt{k^2+m_\ell^2},\end{aligned} \tag{3.27}$$

and

$$\begin{aligned}P &= -\tfrac{1}{2}m_\sigma^2\sigma^2+\tfrac{1}{2}m_\omega^2\omega_0^2+\tfrac{1}{2}m_\rho^2\rho_{03}^2-\tfrac{1}{3}bm_N(g_\sigma\sigma)^3-\tfrac{1}{4}c(g_\sigma\sigma)^4+\\ &+ \tfrac{1}{3}\textstyle\sum_B \frac{2J_B+1}{2\pi^2}\int_0^{k_{F_B}} dk\frac{k^4}{\sqrt{k^2+(m_B-g_{\sigma B}\sigma)^2}}+\\ &+ \tfrac{1}{3}\textstyle\sum_\ell \frac{1}{\pi^2}\int_0^{k_{F_\ell}} dk\frac{k^4}{\sqrt{k^2+m_\ell^2}}.\end{aligned} \tag{3.28}$$

They are the equation of state including strange baryons and they are functions of $n_B=\sum_B n_B$ through the dependence on the Fermi momenta.
As already mentioned, the principal effect caused by hyperon formation in the dense core of neutron stars is a softening of the EOS with a consequent lowering of the maximum mass value. How it will be analyzed in the next chapters, it is possible to observe the softening when compared against the EOS for matter composed of nucleons and leptons alone but using identical assumptions regarding the strong interactions. This basic property of matter with hyperons is a essential result that is basically independent of the precise model used for the baryonic interactions [4].

Chapter 4

The Tolman-Oppenheimer-Volkoff equations

In this chapter we will discuss the last tool needed for the analysis of strange baryon stars: the Tolman-Oppenheimer-Volkoff (TOV) equations.
Through these latter differential equations it is possible to describe the interior structure and, consequently, the main properties of neutron stars. They are the form that Einstein's equations take for spherical static stars, as we will see later.
From the success of Newtonian physics in describing celestial mechanics and other weak gravitational field phenomena, we know that mass is a source of gravity. From the experimental verifications of the Special Theory of Relativity, we also know that all forms of energy are equivalent and must contribute equally as sources of gravity. This is expressed by the famous equation

$$E = mc^2, \tag{4.1}$$

by establishing that mass and energy can transform one into another: they are different manifestations of the same physical quantity.
We will begin our discussion by describing the Newtonian hydrostatic equilibrium of stars. Its subsequent extension to the relativistic case and to the curved space will lead us to define the Einstein's field equations. They tell spacetime how to curve and mass-energy how to configure itself and how to move. Matter acts upon spacetime and in turn is acted upon by spacetime. Moreover, these equations are nonlinear, which means that the gravitational field interacts with itself since the field carries energy, and mass-energy in any form is a source of gravity.
Finally, considering spherical and static stars, the Tolman-Oppenheimer-Volkoff equations are evaluated.

4.1 The Newtonian equilibrium of stellar structure

Consider a nonrelativistic perfect fluid in thermodynamic equilibrium, subject to gravity only. The Euler equation can be written in the form

$$\frac{\partial \boldsymbol{v}}{\partial t} + (\boldsymbol{v} \cdot \boldsymbol{\nabla})\boldsymbol{v} = -\frac{1}{\rho}\boldsymbol{\nabla} P - \boldsymbol{\nabla}\phi, \tag{4.2}$$

where ρ is the density, $\boldsymbol{v}$ is the fluid velocity that is assumed to vary continuosly from point to point, and ϕ is the gravitational potential, satysfing Poisson's equation

$$\boldsymbol{\nabla}^2\phi = 4\pi G\rho, \tag{4.3}$$

where $\boldsymbol{\nabla} = (\frac{\partial}{\partial x}, \frac{\partial}{\partial y}, \frac{\partial}{\partial z})$ and $G = 6.67 \times 10^{-8}$ cm^{3}g^{-1}s^{-2} is the gravitational constant. Eq. (4.2) describes the motion of a fluid in which processes leading to energy dissipation, occuring due to viscosity, i.e. internal friction, and the heat exchange between different regions, can be neglected. For a fluid at rest ($\boldsymbol{v} = 0$), it reduces to

$$\boldsymbol{\nabla} P = -\rho(\boldsymbol{\nabla}\phi). \tag{4.4}$$

For a spherically symmetric fluid, Eqs. (4.3) and (4.4) become

$$\frac{dP}{dr} = -\rho\frac{d\phi}{dr}, \qquad \frac{1}{r^2}\frac{d}{dr}\left(r^2\frac{d\phi}{dr}\right) = 4\pi G\rho. \tag{4.5}$$

Substituting the first of the two above equations into the second, we obtain

$$\frac{1}{r^2}\frac{d}{dr}\left(\frac{r^2}{\rho}\frac{dP}{dr}\right) = -4\pi G\rho, \tag{4.6}$$

$$\frac{dP}{dr} = -\rho(r)\frac{GM(r)}{r^2}, \tag{4.7}$$

with $M(r)$ given by

$$M(r) = 4\pi\int_0^r \rho(r')r'^2 dr'. \tag{4.8}$$

The above result simply states that, at equilibrium, the gravitational force acting on a volume element at distance r from the center of the star is balanced by the force produced by the spacial variation of the pressure.
Given a EOS, Eq.(4.7) can be integrated numerically for any value of the central density to obtain the radius of the star, while thanks to Eq. (4.8) it is possible to evaluate its mass.

4.2 Equilibrium equations in General Relativity

The Newtonian equilibrium equation represents a good approximation when the matter density does not produce an appreciable space-time curvature, in which case the metric is simply given by

$$ds^2 = \eta_{\mu\nu}dx^\mu dx^\nu, \tag{4.9}$$

with

$$\eta = \begin{pmatrix} 1 & 0 & 0 & 0 \\ 0 & -1 & 0 & 0 \\ 0 & 0 & -1 & 0 \\ 0 & 0 & 0 & -1 \end{pmatrix}. \tag{4.10}$$

This tensor, that has already been mentioned in the section (2.2.2), characterizes the flat Minkowski spacetime on which Special Theory of Relativity is based.
The effect of space-time distorsion are negligible when the surface gravitational potential fulfills the requirement $GM/R << 1$. This condition is satisfied by white dwarfs, having $GM/R \sim 10^{-4}$, whose hydrostatic equilibrium can therefore be described as in the previous section. Instead, neutron stars whose larger density leads to much higher values of GM/R, typically $\sim 10^{-1}$, does not satisfy the condition and General Relativity is necessary to describe their interior structure.
In Einstein's theory of General Relativity, Eq. (4.9) is replaced by

$$ds^2 = g_{\mu\nu} dx^\mu dx^\nu, \tag{4.11}$$

where the metric tensor $g_{\mu\nu}$ is a function of space-time coordinates.
The curvature of space-time is described by the *Riemann-Christoffel curvature tensor*

$$R^\rho_{\sigma\mu\nu} = \Gamma^\rho_{\sigma\nu,\mu} - \Gamma^\rho_{\sigma\mu,\nu} + \Gamma^\alpha_{\sigma\nu}\Gamma^\rho_{\alpha\mu} - \Gamma^\alpha_{\sigma\mu}\Gamma^\rho_{\alpha\nu} \tag{4.12}$$

where

$$\Gamma^\lambda_{\mu\nu} = \frac{1}{2} g^{\alpha\lambda}(g_{\alpha\mu,\nu} + g_{\alpha\nu,\mu} - g_{\mu\nu,\alpha}) \tag{4.13}$$

are the *Christoffel symbols* or *affine connections*, in which the notation $V_{\mu\nu,\alpha}$ denotes the ordinary derivative of a covariant tensor $V_{\mu\nu}$: $V_{\mu\nu,\alpha} = \frac{\partial V_{\mu\nu}}{\partial x^\alpha}$.
The metric tensor and the Christoffel symbols are the two essential quantities for General Relativity. This theory is entirely based on two principles:

- the *Equivalence Principle*, stating that in an arbitrary gravitational field, at any given spacetime point, we can choose a locally inertial reference frame such that, in a sufficiently small region surrounding that point, all physical laws take the same form they would take in absence of gravity, namely the form prescribed by Special Relativity;
- the *Principle of General Covariance*, the physical content of which is that if a tensor equation is true in absence of gravity, then it is true in the presence of an arbitrary gravitational field[1].

Following the Equivalence Principle, the metric tensor and affine connections describe the effects of a gravitational field on the motion of falling particle when observed in an arbitrary coordinate frame. This is expressed by the *geodesic equation*

$$\frac{d^2 x^\alpha}{d\tau^2} + \Gamma^\alpha_{\mu\nu}\left[\frac{dx^\mu}{d\tau}\frac{dx^\nu}{d\tau}\right] = 0, \tag{4.14}$$

[1]It should be noted that this Principle can be applied only on scales that are small compared with the typical distances associated to the gravitational field because only on these scales one can construct locally inertial frames.

where τ is the proper time of particle and x^α are the arbitrary frame coordinates. Thus, in analogy with the Newtonian law, we can say that the affine connections are the generalization of the Newtonian gravitational field, and that the metric tensor is the generalization of the Newtonian gravitational potential [15].
Moreover, in addition to these physical meanings, the metric tensor and the affine connections have also important geometrical roles. The first one is a symmetric tensor that allows us to compute the distance (4.11) between two points in any coordinate system, and so it characterizes the spacetime geometry. Moreover, defining the inverse metric $g^{\mu\nu}$ as

$$g^{\mu\alpha}g_{\alpha\nu} = \delta^\mu{}_\nu, \tag{4.15}$$

allow us to raise and lower a tensor index through

$$A^\mu{}_\nu = g^{\mu\alpha}A_{\alpha\nu}. \tag{4.16}$$

On the other hand, the affine connections can be used to compute the derivative of a vector in an arbitrary space. This is known as covariant derivative and the notation used to indicate it is

$$V_{\mu;\nu} = \frac{dV_\mu}{dx^\nu} - \Gamma^\lambda_{\mu\nu}V_\lambda. \tag{4.17}$$

When spacetime is flat, $g_{\mu\nu}$ has the Minkowski metric form and from Eq. (4.13) the $\Gamma^\lambda_{\mu\nu}$, containing the metric tensor derivative, vanishes in this frame in all spacetime. Consequently, also its derivatives do it. Therefore the Riemann tensor vanishes everywhere at all times in flat spacetime. Since this is a statement about a tensor, according to the Principle of General Covariance, it is true in any coordinate system. This is why the Riemann tensor deserves its name of curvature tensor: only when the space is curved it assumes a non-zero value. Indeed the Riemann tensor is the only one that can be constructed from the metric tensor and its first and second derivatives, and which is linear in the second derivatives. This last property is the fundamental one. In fact when we consider a curved space, thanks to the Equivalence Principle, we can always choose at each point of spacetime a coordinate system such that $g_{\mu\nu}$ reduces to $\eta_{\mu\nu}$. In that case as already mentioned $\Gamma^\lambda_{\mu\nu}$ vanishes but consequently in the Riemann tensor only the non-linear part vanishes as well.
From equation (4.12) it is possible to derive the simmetry properties of the tensor

$$\begin{aligned} R^\mu_{\nu\rho\sigma} &= -R^\mu_{\nu\sigma\rho}, \\ R^\alpha_{\nu\rho\sigma} + R^\alpha_{\sigma\nu\rho} + R^\alpha_{\rho\sigma\nu} &= 0. \end{aligned} \tag{4.18}$$

Lowering the index, we obtain $R_{\rho\sigma\mu\nu} = g_{\rho\alpha}R^\alpha_{\sigma\mu\nu}$ from which the additional symmetries follow:

$$\begin{aligned} R_{\mu\nu\rho\sigma} &= -R_{\nu\mu\rho\sigma} = -R_{\mu\nu\sigma\rho}, \\ R_{\mu\nu\rho\sigma} &= R_{\rho\sigma\mu\nu} = R_{\sigma\rho\nu\mu}. \end{aligned} \tag{4.19}$$

As consequence of the symmetries only 20 of the 4^4=256 components of Riemann tensor are independent.
Moreover, from this tensor, other two important objects can be obtained, the *Ricci tensor*

$$R_{\mu\nu} = R^\rho_{\mu\nu\rho}\,, \tag{4.20}$$

and the *scalar curvature*

$$R = g^{\mu\nu} R_{\mu\nu}. \tag{4.21}$$

According to its definition as a contraction of the Riemann tensor, the Ricci tensor can be written

$$R_{\mu\nu} = \Gamma^{\alpha}_{\mu\alpha,\nu} - \Gamma^{\alpha}_{\mu\nu,\alpha} - \Gamma^{\alpha}_{\mu\nu}\Gamma^{\beta}_{\alpha\beta} + \Gamma^{\alpha}_{\mu\beta}\Gamma^{\beta}_{\nu\alpha}. \tag{4.22}$$

These two latter quantities will be fundamental to determine the TOV equations.
In addition to the symmetry properties discussed above, the Riemann tensor also satisfies the differential equations known as the *Bianchi identities*

$$R^{\alpha}_{\mu\nu\rho;\sigma} + R^{\alpha}_{\mu\sigma\nu;\rho} + R^{\alpha}_{\mu\rho\sigma;\nu} = 0. \tag{4.23}$$

By multiplying the Bianchi identities by $g^{\mu\nu}$ and using the Riemann tensor simmetries and the fact that the covariant derivative of the metric tensor is zero, we arrive at the vanishing divergence

$$(R^{\mu\nu} - \frac{1}{2} g^{\mu\nu} R)_{;\nu} = 0. \tag{4.24}$$

The object in the brackets is called the *Einstein tensor* and its covariant form is

$$G_{\mu\nu} = R_{\mu\nu} - \frac{1}{2} g_{\mu\nu} R. \tag{4.25}$$

This tensor is symmetric and of second rank. Moreover, it is a linear homogeneous combination of terms linear in the second derivative or quadratic in the first, in analogy with Poisson's equation for the gravitational potential in Newton's theory (4.3).
The most general expression of Einstein's tensor that includes the mass-energy properties of the material medium, thanks to a second rank symmetric divergenceless tensor $T_{\mu\nu}$, is

$$G_{\mu\nu} = kT_{\mu\nu} + \Lambda g_{\mu\nu}, \tag{4.26}$$

where Λ is the so-known cosmological constant. It was not present in the original theory and was added to obtain a static cosmology before it was known that the universe is expanding. It is sometimes referred to as the vacuum energy density. In any case it is small, the current value is $\Lambda \approx 1.11 \times 10^{-56}\,\mathrm{cm}^{-2}$ [15] and its effect is cosmological, the stellar structure is not affected by it, so it will be neglected.
Thus the set of differential equations (4.26) determine the gravitational fields $g_{\mu\nu}$ inside a spacetime region of mass-energy and in addition determine how the mass-energy is arranged by gravity. With appropriate $T_{\mu\nu}$ it would provide the equations of stellar structure. The constant k can be fixed by looking to the weak and stationary field limit where the General Theory of Relativity should agree with Newton's field theory, as demonstrated in Appendix B. Therefore, they read

$$G_{\mu\nu} = -8\pi G T_{\mu\nu}. \tag{4.27}$$

We remark the fact that the Einstein field equations are nonlinear in the fields $g_{\mu\nu}$ since both mass and energy are sources of gravitational field that carries energy and therefore, it interacts with itself.
Although Einstein equations appear to be simple, nonlinearity makes them particularly difficult to solve, as does the fact that spacetime acts on mass and vice versa. However, there are specific cases in which the solutions of the equations can be obtained in closed form.

4.2.1 TOV equations determination

When the interior structure of a spherical static star is considered, the coupled differential Einstein equations can be calculated numerically and they are called the Tolman-Oppenheimer-Volkoff equations.
In this case the spacetime is static and isotropic, so the $g_{\mu\nu}$ are independent of time and $g_{0i} = 0$. Moreover, we also consider that matter in the star is in chemical, hydrostatic and thermodynamic equilibrium.
The metric of the corresponding gravitational field can be written in the form $(x^0 = t, x^1 = r, x^2 = \theta, x^3 = \phi)$

$$ds^2 = g_{\mu\nu}dx^\mu dx^\nu = e^{2\nu(r)}dt^2 - e^{2\lambda(r)}dr^2 - r^2d\theta^2 - r^2\sin^2\theta d\phi^2 \tag{4.28}$$

implying

$$g = \begin{pmatrix} e^{2\nu(r)} & 0 & 0 & 0 \\ 0 & -e^{2\lambda(r)} & 0 & 0 \\ 0 & 0 & -r^2 & 0 \\ 0 & 0 & 0 & -r^2\sin^2\theta \end{pmatrix}, \tag{4.29}$$

$\nu(r)$ and $\lambda(r)$ being functions only of r and to be determined solving Einstein equations. In order to construct the Einstein tensor for the interior of the star, we need both the Ricci tensor and scalar curvature.
We can derive the nonvanishing affine connections (4.13), which are symmetric in their lower indices, from the metric tensor that has just been calculated

$$\begin{aligned} &\Gamma^1_{00} = \nu' e^{2(\nu-\lambda)}, && \Gamma^0_{10} = \nu', \\ &\Gamma^1_{11} = \lambda', && \Gamma^2_{12} = \Gamma^3_{13} = 1/r, \\ &\Gamma^1_{22} = -re^{-2\lambda}, && \Gamma^3_{23} = \cot\theta, \\ &\Gamma^1_{33} = -r\sin^2\theta e^{-2\lambda}, && \Gamma^2_{33} = -\sin\theta\cos\theta. \end{aligned}$$

The primes denote differentiation with respect to coordinate r. Thus, for static isotropic spacetime, the components of Ricci tensor (4.20) are

$$\begin{aligned} R_{00} &= \left[-\nu'' + \lambda'\nu' - \nu'^2 - \frac{2\nu'}{r}\right]e^{2(\nu-\lambda)} \\ R_{11} &= \nu'' - \lambda'\nu' + \nu'^2 - \frac{2\lambda'}{r} \\ R_{22} &= (1 + r\nu' - r\lambda')e^{-2\lambda} - 1 \\ R_{33} &= R_{22}\sin^2\theta, \end{aligned} \tag{4.30}$$

and the scalar curvature (4.21) reads

$$\begin{aligned} R = g^{\mu\nu}R_{\mu\nu} &= e^{-2\nu}R_{00} - e^{-2\lambda}R_{11} - \frac{2}{r^2}R_{22} \\ &= e^{-2\lambda}\left[-2\nu'' + 2\lambda'\nu' - 2\nu'^2 - \frac{2}{r^2} + 4\frac{\lambda'}{r} - 4\frac{\nu'}{r}\right] + \frac{2}{r^2}. \end{aligned} \tag{4.31}$$

Under the standard assumption that matter in the star interior behave as an ideal fluid, the energy-momentum tensor describing the distribution of matter can be

written in the form already encountered in section (2.2.2) that generalized is

$$T_{\mu\nu} = u_\mu u_\nu(\epsilon + P) - g_{\mu\nu}P. \tag{4.32}$$

Of course, also in this case, ϵ and P denote energy density and pressure, respectively, and u_μ the local four-velocity that, with the hypotesis that fluid is at rest, in this case is given by

$$1 = u_\mu u_\nu g^{\mu\nu} = (u_0)^2 g^{00} \Rightarrow u_\mu = (e^{\nu(r)}, 0, 0, 0)\,, \tag{4.33}$$

where $g^{00} = e^{-2\nu(r)}$ is evaluated thanks to the relation (4.15). The explicit form of the energy-momentum tensor is

$$T_{\mu\nu} = diag(\epsilon e^{2\nu}, Pe^{2\lambda}, Pr^2, Pr^2\sin^2\theta), \tag{4.34}$$

unlike the flat spacetime case in which it is simply $T_{\mu\nu} = diag(\epsilon, P, P, P)$ by using $u_\mu = (1, 0, 0, 0)$ and the Minkowski metric.
Substitution of Eqs. (4.34), (4.30) and (4.31) into Einstein field equation (4.27), with the definition of Einstein tensor (4.25), leads to the system of differential equations

$$\begin{aligned}
G_{00} &\equiv e^{-2\lambda}\left(\frac{1}{r^2} - \frac{2\lambda'}{r}\right) - \frac{1}{r^2} = -8\pi G\epsilon(r),\\
G_{11} &\equiv e^{-2\lambda}\left(\frac{1}{r^2} + \frac{2\nu'}{r}\right) - \frac{1}{r^2} = 8\pi GP(r),\\
G_{22} &\equiv e^{-2\lambda}\left(\nu'' + \nu'^2 - \lambda'\nu' + \frac{\nu' - \lambda'}{r}\right) = 8\pi GP(r),\\
G_{33} &\equiv G_{22} = 8\pi GP(r).
\end{aligned} \tag{4.35}$$

where $\epsilon(r)$ and $P(r)$ denote the space distribution of energy density and pressure, respectively. The last equation provides no additional information to that provided by those preceding it.
The above equations can be cast in the form originally derived by Tolman, Oppenheimer and Volkoff [1], [16]

$$\frac{dP(r)}{dr} = -\epsilon(r)\frac{GM(r)}{r^2}\left[1 + \frac{P(r)}{\epsilon(r)}\right]\left[1 + \frac{4\pi r^3 P(r)}{M(r)}\right]\left[1 - \frac{2GM(r)}{r}\right]^{-1}, \tag{4.36}$$

where

$$M(r) = 4\pi\int_0^r \epsilon(r)r^2 dr \tag{4.37}$$

is the *included* mass within the coordinate r. It is interesting to note that since of the mutual interaction of mass-energy and spacetime, talking about the "mass of the star" has no meaning in isolation from the field energy. In fact M is often referred to as the *gravitational* mass or the mass-energy of the star. Consequently, even if Eqs. (4.8) and (4.37) have the same form, they represent different quantities: nonrelativistic (4.8) denotes the mass whose distribution is given by matter density ρ, while (4.37) comprises the mass of the star and its gravitational field.
Instead, observing the Eq. (4.36), the first term in the right hand side is the newtotian gravitational force. It is the same as the one appearing in Eq. (4.7), but

with matter density replaced by energy density. The first two additional terms take into account relativistic corrections, that become vanishingly small in the limit $k_F/m \to 0$, m and k_F being the mass and Fermi momentum of the star constituents, respectively. Lastly, the third factor indicates the effect of spacetime curvature. Of course, in the nonrelativistic limit Eq. (4.36) reduces to the classical equilibrium equation (4.7).

The TOV equations express the balance at each r between the internal pressure and gravitational attraction of the mass-energy interior to r. They are the equations of hydrostatic equilibrium in General Relativity.

Given an equation of state in the form $\epsilon = \epsilon(P)$ or $P = P(\epsilon)$, the stellar structure equations (4.36) and Eq. (4.37) can be solved simultaneously for the radial distribution of pressure, $P(r)$, and of mass-energy density $\epsilon(r)$. Because the TOV equations, supplemented with EOS, consist of two first-order, ordinary differential equations, they require two boundary conditions at some point, respectively on $M(r)$ and $P(r)$, for instance at the center of the star. In order to evaluated the boundary condition on M, consider a tiny sphere of radius $r = x$. The proper circumference is $2\pi x$ and the proper radius is

$$\int_0^x e^{\lambda} dr \simeq e^{\lambda} x, \tag{4.38}$$

so their ratio is $2\pi e^{-\lambda}$. Since, by the Equivalence Principle, the spacetime is locally flat the ratio between the circumference of this infinitesimal sphere and the radius must be 2π. This implies that $e^{\lambda} \to 1$ as $r \to 0$. Now if we write the first equation of (4.35) in the form

$$r^2 G_{00} = -\frac{d}{dr}[r(1 - e^{-2\lambda(r)})] = -8\pi G r^2 \epsilon(r) \tag{4.39}$$

this can be integrated to yield

$$e^{-2\lambda(r)} = 1 - \frac{8\pi G}{r} \int_0^r \epsilon(r) r^2 dr. \tag{4.40}$$

Using the above equation to replace the integral in Eq. (4.37), we obtain

$$M(r) = \frac{r}{2G}\left(1 - e^{-2\lambda(r)}\right). \tag{4.41}$$

As $e^{\lambda} \to 1$ it follows from above equation that $M(0) = 0$. Therefore, the Tolman-Oppenheimer-Volkoff equations can be integrated from the origin with initial conditions $M(0) = 0$ and an arbitrary value for the central energy density $\epsilon(0) = \epsilon_c$, for which we have $P(r = 0) = P(\epsilon_c)$, until the pressure $P(r)$ becomes zero at R, the radius of the star. R is the radial coordinate exterior to which the pressure vanishes. Zero pressure provides the edge of the star because it can support no overlying matter against the gravitational attraction. The corresponding value of $M \equiv M(R)$ denotes the gravitational mass of star.

For the given equation of state, there is only one relationship between M and ϵ_c. So for each possible EOS, there is a unique family of stars, parametrized by central density, and it is referred to as the *single parameter sequence* of stars corresponding to the given equation of state.

4.2.2 Limiting mass

The relevant role in the structure of relativistic stars is played by pressure, that in addition to supporting them against the matter compression produced by gravity, also assures the gravitational collapse of relativistic stars whose mass is above a certain limit.
Pressure appears together with energy density on the right side of equation (4.36) in determining the monotonic decrease of pressure as the distance from the centre of the relativistic star increases. The fact that the pressure gradient is negative makes sense because the quantity of overlaying matter decreases with radial coordinate, i.e. the greatest weights are at the center and decreases in the outward direction. Thus, when the mass of a relativistic star increases, the supporting pressure must correspondingly increase to resist a greater gravitational force and its negative gradient becomes larger in magnitude, making the radius of the star smaller because its edge occurs at $P = 0$. Consequently, when the mass of a relativistic star exceeds a critical value, there is no escape from gravitational collapse to a black hole. Whatever the EOS, the one-parameter sequence of stable configurations belonging to that equation of state is ended by a maximum-mass compact star. The mass of this star is referred to as the *mass limit* or *limiting mass* of the sequence.
So smaller the mass, the less the gravitational attraction and the larger the radius. In neutron stars with intermediate mass, the Fermi pressure of nucleons and their mutual repulsion when in close vicinity resists gravity, leading to a range of masses for which the radius hardly changes. Finally, as the limiting mass is reached, the radius decreases significantly with mass. This important relationship between the mass of relativistic star and its radius is known as *mass-radius relation.*
Finally, the limiting mass of a model sequence of stars depends on the compressibility of matter, which is registered in the equation of state. A "soft" equation of state is relatively easier to compress than a "stiff" one. The stiffer the equation of state, the larger the mass that can be sustained against collapse. When the hyperons appear, being driven by Pauli principle in dense matter, they lower Fermi energies of baryons and hence the total energy. The pressure, which resists gravitational collapse, is also reduced. Therefore hyperons soft he EOS and the limiting neutron star mass is reduced in comparison with models in which strange baryons are omitted.

4.2.3 A necessary condition for the stability of a compact star

The solution of TOV equations with the appropriate boundary conditions describes the hydrostatic equilibrium of a star. However, equilibrium does not assure stability and its configurations may correspond either to a maximum or to a minimum in the energy with respect to radial compression or expansion. Now we briefly discuss how to determine if an equilibrium configuration is stable or not.
Let us assume to have numerically integrated the TOV equations with an assigned equation of state for any value of the central energy density ϵ_c and thus have obtained the profile of function $M(\epsilon_c)$. The typical form of this profile is shown in the figure 4.1, in which each point represent an hydrostatic equilibrium configuration. Consider a compact star in the equilibrium configuration A, as well as labeled in figure 4.1. Now suppose that this solution is perturbed so that the central density ϵ_c is increased:

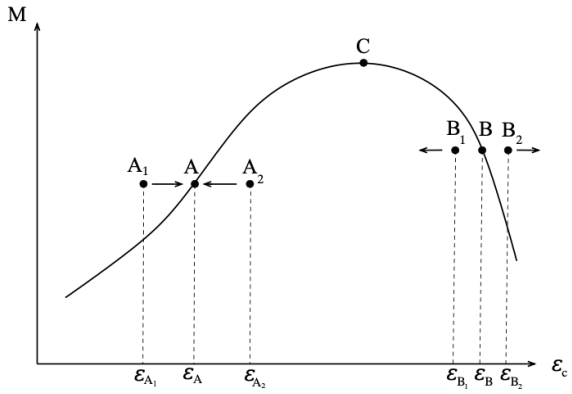

Figure 4.1. Gravitational mass of a compact star in hydrostatic equilibrium configurations as a function of the central energy density.

the central energy density ϵ_{A_2} leaving the mass unchanged and the new configuration of non-equilibrium is A_2. Now the mass of the star is below the value required for hydrostatic equilibrium, therefore the pressure exceeds gravity and provides a further expansion that raises up the density and brings the star again in an equilibrium configuration.
Similarly, if a small radial perturbation decreases the central density to ϵ_{A_1} leaving the mass unchanged and so the star has a mass that is above the value necessary to reach an equilibrium configuration. Thus the gravitational attraction exceeds the pressure gradient and provides a further contraction that increases the energy density until its equilibrium value is reached.
From the points discussed above, we can conclude that A is a *stable* equilibrium configuration and the condition for stability is

$$\frac{dM(\epsilon_c)}{d\epsilon_c} > 0. \tag{4.42}$$

A similar discussion can be done about the point B in Fig. 4.1, where

$$\frac{dM(\epsilon_c)}{d\epsilon_c} < 0. \tag{4.43}$$

In this case a displacement to the configuration B_1 leads to a gravity weaker than the internal pressure and therefore the star expands reducing the central energy density. On the other hand, the displacement to the configuration B_2 provides a further contraction that indefinitely increases the central density. Therefore the equilibrium in B is *unstable*.
Observing the Fig. 4.1, in which the point C indicates the configuration of maximum mass, the branch of the curve on the left of this point corresponds, in principle, to stable configurations, whereas that on the right to unstable configurations.
However, it should be stressed that the stability condition for a static, spherically symmetric star that has been found is only necessary but not sufficient. The reason can be understood by treating the full theory of radial and non-radial perturbations of a star but it is outside the scope of this work.

Chapter 5

Results

In this chapter we will present and discuss the results of numerical calculations of the equation of state and TOV equations performed by two *Fortran* computational codes.
The first program (1P) to evaluated the EOS has been implemented specifically for this work. The code takes as input the five parameters of the Lagrangian of the relativistic theory discussed at the end of chapter 2: g_σ/m_σ, g_ω/m_ω, g_ρ/m_ρ, b and c. Then it generates as output the values of the main quantities necessary for the analysis of the stellar structure: energy density (ϵ) and pressure (P), nucleon effective mass (m_N^*), binding energy per nucleon (B/A), compression modulus (K), symmetry energy coefficient (a_{sym}) and i-particle fraction (x_i). All these quantities are computed as function of baryon density (n_B).
The program (2P) to integrate the differential TOV equations, taking as input the energy density ϵ and the pressure P values produced from the first computational code, is based on a fourth ordered Runge-Kutta algorithm. The integration was carried out on the radial variable r and it was employed a variable integration step in order to accomodate strongly variable functions. Such a step is given by:

$$\Delta r = \Delta \cdot \left(\frac{1}{M}\frac{dM}{dr} - \frac{1}{P}\frac{dP}{dr} \right)^{-1}, \tag{5.1}$$

where Δ is an arbitrary scale parameter, that we put to $\Delta = 0.05$ as it was a good compromise to have a great efficiency.
In the following sections we will analyze the results obtained for the model that includes only nucleons and then that in which the hyperon Λ is present. Of course, with regard to the 1P code, in strange matter case other parameters in addition to five mentioned above must be necessary inserted as we will discuss.

5.1 Non-strange matter case

In order to obtain the explicit dependence of equation of state on the baryon density, the Eqs. (2.56) and (2.57) are recast in the following form

$$\begin{aligned}\epsilon(n_p,n_n) &= \tfrac{1}{2}\tfrac{m_\sigma^2}{g_\sigma^2}(m_N-m_N^*)^2+\tfrac{1}{2}\tfrac{g_\omega^2}{m_\omega^2}n_B^2+\tfrac{1}{8}\tfrac{g_\rho^2}{m_\rho^2}(n_p-n_n)^2\\ &+ \tfrac{b}{3}m_N(m_N-m_N^*)^3+\tfrac{c}{4}(m_N-m_N^*)^4+\\ &+ \tfrac{1}{\pi^2}\textstyle\sum_{i=p,n}\int_0^{k_{F_i}}k^2dk\sqrt{|\mathbf{k}|^2+m^{*2}},\end{aligned} \tag{5.2}$$

and

$$\begin{aligned}P(n_p,n_n) &= -\tfrac{1}{2}\tfrac{m_\sigma^2}{g_\sigma^2}(m_N-m_N^*)^2+\tfrac{1}{2}\tfrac{g_\omega^2}{m_\omega^2}n_B^2+\tfrac{1}{8}\tfrac{g_\rho^2}{m_\rho^2}(n_p-n_n)^2\\ &- \tfrac{b}{3}m_N(m_N-m_N^*)^3-\tfrac{c}{4}(m_N-m_N^*)^4+\\ &+ \tfrac{1}{3\pi^2}\textstyle\sum_{i=p,n}\int_0^{k_{F_i}}dk\tfrac{k^4}{\sqrt{k^2+m^{*2}}}\end{aligned} \tag{5.3}$$

These expressions are obtained using the relation of nucleon effective mass (2.23) and the equations of motion of mesons σ, ω and ρ (2.45)-(2.47), considering $k_F = (3\pi n)^{1/3}$.
We start our analysis choosing four sets of parameters to characterize the model. They are reported in Table 5.1.

	$(g_\sigma/m_\sigma)^2$ [GeV^{-2}]	$(g_\omega/m_\omega)^2$ [GeV^{-2}]	$(g_\rho/m_\rho)^2$ [GeV^{-2}]	b	c
S1 [17]	405.44	310.61	109.98	0	0
S2 [6]	394.831	300.460	87.398	0	0
S3 [18]	302.93	183.68	113.29	0.00295	-0.00107
S4 [12]	257.78	137.54	159.27	0.00414	0.00716

Table 5.1. The four sets used for the model.

Thus we verify that the two main nuclear properties, i.e. the saturation density and the binding energy per nucleon, are in agreement with the empirical values in the case of isospin symmetric matter ($n_p = n_n$). As it has been mentioned in Chapter 2, these two properties are essential to correctly develop any theoretical model to describe stellar matter. In Fig. 5.1 we show the behavior of the binding energy per nucleon as function of density number for the four different parameter sets. The analytical parametrization of this quantity is

$$\left[\frac{B}{A}\right](n_B) = \frac{\epsilon}{n_B} - m_N\,. \tag{5.4}$$

The graph shows that the four curves reach their minimum, i.e. the saturation point,

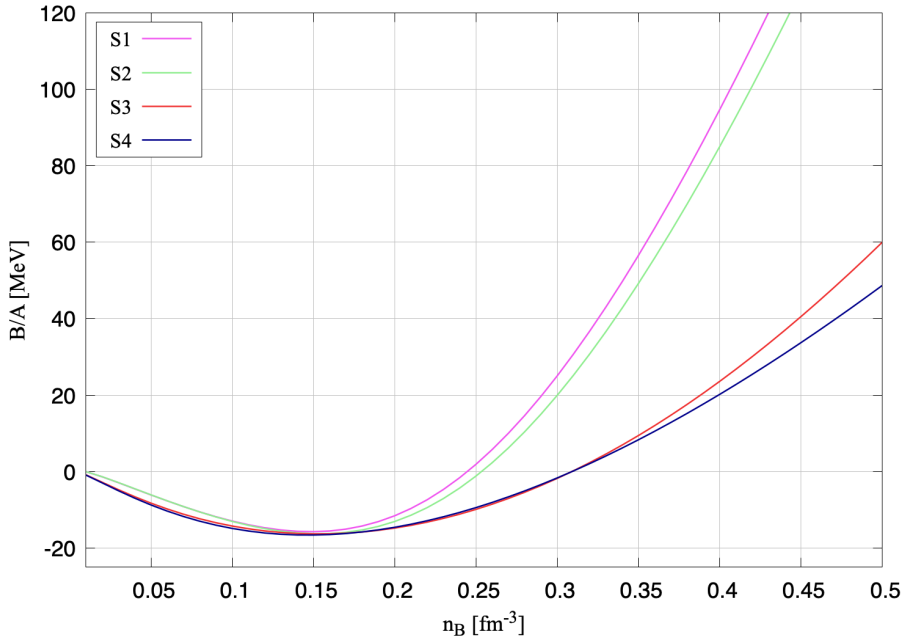

Figure 5.1. Binding energy per nucleon trend in function of baryon density for the four sets of parameters reported in Table 5.1 in isospin symmetric matter.

at density $n_0 \sim 0.15$ fm^{-3} that is in good agreement with the empirical saturation density value (2.3). At this density, the binding energy per nucleon in the four cases takes the value reported in Table 5.2 and also these numerical results are compatible with (2.3).

	S1	S2	S3	S4
$(B/A)_{n_0}$ [MeV]	-15.8	-16.3	-16.3	-16.6

Table 5.2. B/A at saturation density for each case.

For isospin symmetric nuclear matter at the saturation density, nucleons are in bound states with a soft equilibrium between medium range attraction and short range repulsion provided by scalar σ and vector meson ω, respectively. Thus the system is in its ground state and all energy levels are occupied by neutrons and protons up to Fermi energies $E_F^* = \sqrt{k_F^2 + m_N^{*2}} + g_\omega \omega^0 \sim 760$ MeV.
In S1 and S2 cases, in which the self-interaction parameters of scalar meson σ are set to zero we note that binding energy increases faster than other two cases. In the absence of the self-interaction terms the balance between repulsion and attraction is lost first in favor of repulsion and as a consequence, the system leaves the saturation region earlier than when such terms are present.
Moreover, it should be noted that for S3 case, since c is negative, the energy density (5.2) is unbounded from below for a large enough scalar field. This is not allowed for a quantum field theory, but we work by taking the view that the theory is effective,

considering as degrees of freedom composite particles and not fundamental ones. In this circumstance if specific parameters are taken into account, the saturation properties of nuclear matter are reproduced in good way and a reasonable behavior of the EOS is assured in the proximity of saturation. For the specific S3 case, the saturation density and binding energy per nucleon are well reproduced as discussed above.
After discussing the two fundamental nuclear properties, we focus on the equation of state that describe the pressure as function of baryon density (5.3). The profile of this EOS for isospin symmetric nuclear matter is shown in Figure 5.2, where the results extracted from heavy-ion experimental data [19] are also plotted.

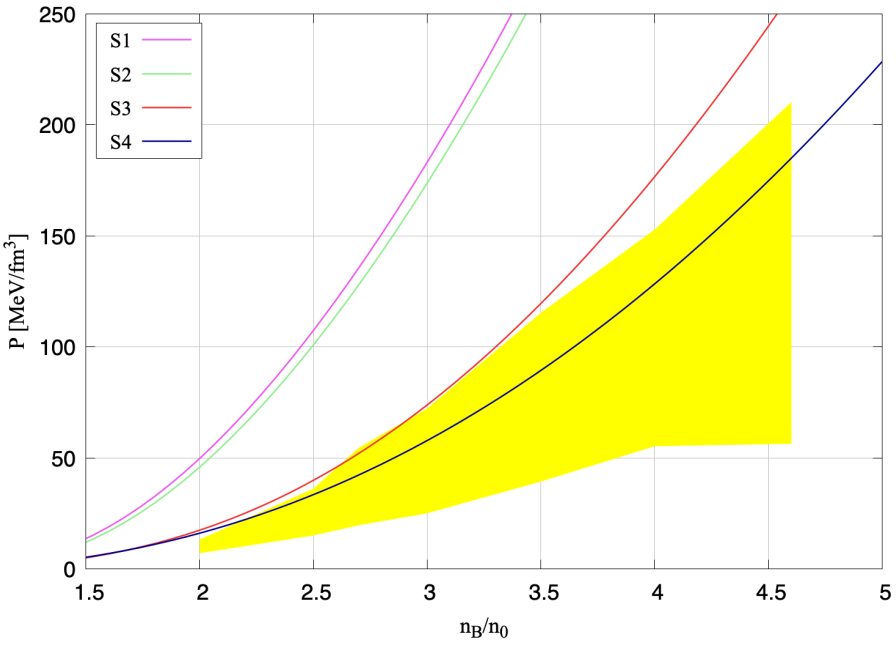

Figure 5.2. Pressure as a function of the ratio between baryon and saturation densities for the four parameter sets. The yellow shaded area corresponds to the region consistent with the experimental data reported in Ref. [19].

Looking at the graph it is evident that only the curve related to the S4 parameter set is compatible with the experimental constraints. For this reason, the following analysis is performed by using only this set. To understand why the other sets reproduce not optimal equations of state it is necessary to consider the structure of (5.3). At low density, below the saturation density, the theory is not of interest because the nuclear matter behaves like a a nonrelativistic ideal Fermi gas. Instead, at higher density above the saturation, the pressure increases very strongly and the equation of state starts to converge to [6]

$$\begin{aligned} P(n_B) \rightarrow & \frac{1}{2}\frac{g_\omega^2}{m_\omega^2}n_B^2 - \frac{m_\sigma^2}{g_\sigma^2}\frac{m_N^2}{2} - bm_N\frac{m_N^3}{3} - c\frac{m_N^4}{4} \\ & + \frac{m_\sigma^2}{g_\sigma^2}m_N m_N^* + bm_N^3 m_N^* + cm_N^3 m_N^* + O\left[\left(\frac{m_N^*}{m_N}\right)^2\right]. \end{aligned} \tag{5.5}$$

The leading term for the pressure increase is the first that comes from the strong repulsion caused by the vector meson ω exchange.Then, the following three negative terms provide a reduction of the pressure and they come from the attraction generated by the exchange of scalar meson σ. The last three positive terms are the first relativistic corrections of the previous terms and slightly increase the strength of the scalar interactions.
Thus for S1 and S2 sets, the absence of scalar self-interactions (i.e. of third, fourth, sixth and seventh term of (5.5)) leads to have a lower attenuation of the effect of the ω repulsion and therefore to a steeper increase of the pressure. On the other hand, for S3 set where the self-interaction is present, the trend of the pressure is better of the previous cases but the negative value of c does not make it compatible with the experimental data. This can be explained by observing that the change of sign affects both the fourth term and its first order relativistic correction, i.e. the seventh term. Between the two, the one that leads to a greater contribution to the pressure is certainly the third term that therefore causes a slightly faster increase in pressure.
With the selected S4 set, we complete the study of the nuclear properties by calculating the symmetry energy coefficent, compressibility and the effective mass at saturation density for symmetric matter.
The first quantity is related to the equation of state (5.2) by

$$a_{sym} = \frac{1}{2}\left(\frac{\partial^2(\epsilon/n_B)}{\partial t^2}\right)_{t=0} \qquad , \qquad t \equiv \frac{n_p - n_n}{n_B}. \tag{5.6}$$

By expressing n_p and n_n in term of t and n_B and making the indicated derivatives, after some algebra, we obtain [6]

$$a_{sym} = \frac{k_F^2}{6E_F^*} + \frac{1}{8}\left(\frac{g_\rho^2}{m_\rho^2}\right)n_B \tag{5.7}$$

The first term derives from the difference between the Fermi energies of protons and neutrons. The second one results from the isospin coupling between the ρ meson and the nucleons. These two terms together assure that neutrons and protons have the same Fermi energy.
The numerical value evaluated at saturation density is

$$a_{sym} = 30.77\,\mathrm{MeV}\,, \tag{5.8}$$

that is compatible with its empirical value (2.4).
The expression of compression modulus (2.6) related to (5.3), for isospin symmetric case, can be parameterized as [6]

$$\begin{aligned} K = \frac{3k_F^2}{E_F^*} + \frac{6}{\pi^2}\frac{g_\omega^2}{m_\omega^2}k_F^3 - 6\frac{g_\sigma^2}{m_\sigma^2}\frac{k_F^3 m_N^{*2}}{\pi^2 E_F^{*2}}\left(1 + \frac{g_\sigma^2}{m_\sigma^2}\left\{2bm_N^* g_\sigma\sigma\right.\right. \\ \left.\left. + 3cg_\sigma^2\sigma^2 + \frac{2}{\pi}\left[\frac{k_F^3 + 3k_F m_N^{*2}}{2E_F^*} - \frac{3}{2}m_N^{*2} ln\left(\frac{E_F^* + k_F}{m_N^*}\right)\right]\right\}\right)^{-1}. \end{aligned} \tag{5.9}$$

At saturation, the numerical result obtained is

$$K = 231.75\,\mathrm{MeV}, \tag{5.10}$$

that is in the typical validity range of this quantity $220 - 260$ MeV and indicates that the equation of state for the chosen coupling parameters is soft.
Finally, we evaluate the last important nuclear quantity, i.e. the ratio

$$\frac{m_N^*}{m_N} = 0.767 \tag{5.11}$$

and it is also compatible with empirical limits discussed in section 2.1.
After these considerations we consider the β-stable nuclear matter. The β equilibrium and charge neutrality conditions for a system $npe\mu$ are that shown in chapter 4. At low density, the system is composed only of neutrons and an equal number of protons and electrons $n_p = n_e$ in order to have charge neutrality. As the baryon density increases, when the condition $\mu_e = \mu_\mu$ is satisfied the muons appear and the zero electrical charge relation becomes $n_p = n_e + n_\mu$. In the model that we consider, the chemical potentials of protons and neutrons necessary to beta equilibrium have a different dependence from their Fermi momenta k_F. This is due to their different effective interactions with scalar and vector mesons, especially with the meson ρ for the different 3-component of the isospin. Consequently it is possible to define an *effective* chemical potential for proton and neutron

$$\mu_N^* = \sqrt{k_F^2 + m_N^{*2}} + \frac{g_\omega^2}{m_\omega^2} n_B \pm \frac{1}{4}\frac{g_\rho^2}{m_\rho^2}(n_p - n_n). \tag{5.12}$$

The composition of the β-stable nuclear matter is reported in Fig. 5.3.

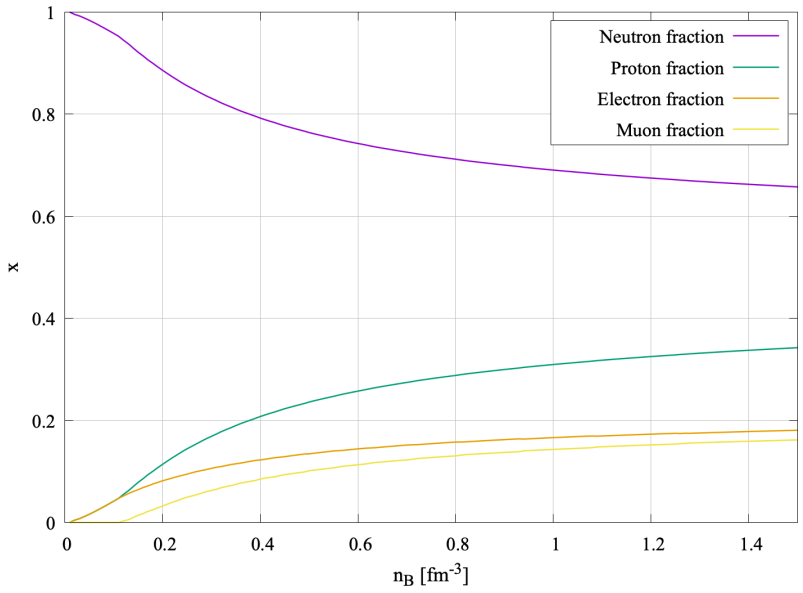

Figure 5.3. Concentrations of the different nuclear matter constituents in beta equilibrium as a function of the baryon density.

At density ~ 0.12 fm^{-3} the electron and muon chemical potentials become equal and muons start to appear. With this configuration, in order to integrate the Tolman-Oppenheimer-Volkoff equations and evaluate the characteristic mass-radius

relation, we recast the equation of state in the $P(\epsilon)$ form where explicit dependence on total baryon density disappears. This form can be reached by inverting the equation (5.2) and replacing the obtained expression for n_B into (5.3):

$$\begin{aligned} P(\epsilon) &= \epsilon - \frac{m_\sigma^2}{g_\sigma^2}(m_N - m_N^*)^2 - \frac{2}{3}bm_N(m_N - m_N^*)^3 - \frac{c}{2}(m_N - m_N^*)^4 + \\ &+ \frac{1}{3\pi^2}\sum_{i=p,n}\int_0^{k_{F_i}} dk \frac{k^4}{\sqrt{k^2+m_N^{*2}}} \\ &- \frac{1}{\pi^2}\sum_{i=p,n}\int_0^{k_{F_i}} k^2 dk \sqrt{|\mathbf{k}|^2 + m_N^{*2}}. \end{aligned} \tag{5.13}$$

The behavior of the pressure as function of energy density is shown in Fig. 5.4.

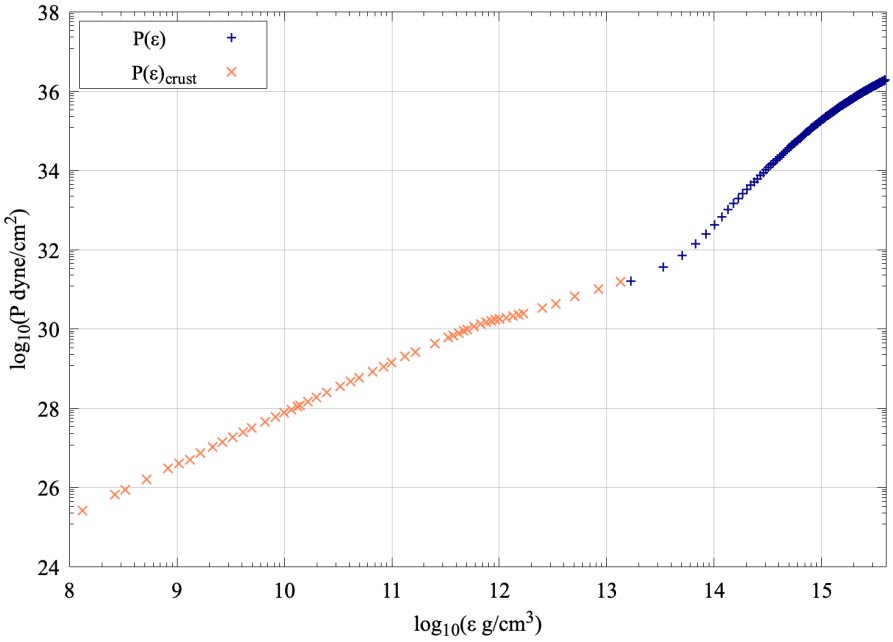

Figure 5.4. Equation of state (blue) computed with the 1P computational code using S4 parameter set. At energy density $\lesssim 2 \times 10^{13}$ g/cm^3 such equation of state is replaced by the crust EOS (orange) taken from Ref. [20].

At small densities the equation of state computed by 1P program is substituted with the crust EOS proposed in Ref. [20]. The replace of the EOSs occurs at density $\sim 0.1 n_0$ where $\epsilon \sim 2 \times 10^{13}$ g/cm^3 and $P \sim 1.6 \times 10^{31}$ dyne/cm^2.
Finally, by using the data plotted in Fig. 5.4 as input for 2P program, the TOV equations are solved. This integration provides numerical results to define mass-radius relation whose trend is shown in Fig. 5.5.
The maximum mass reached is $\sim 2.18\, M_\odot$ at $R \sim 11.6\, km$, that is compatible with the constraints of recent measurements $M_{max} = 2.27^{+0.17}_{-0.15}\, M_\odot$ [21], as illustrated in the figure.
It should be noted that the crust of a neutron star contributes only about one percent to the mass and so the main impact of crust EOS is in the tail of the mass curve.
In the next section we will discuss how the equation of state and, consequently, the mass-radius diagram changes with the hyperon Λ appearance.

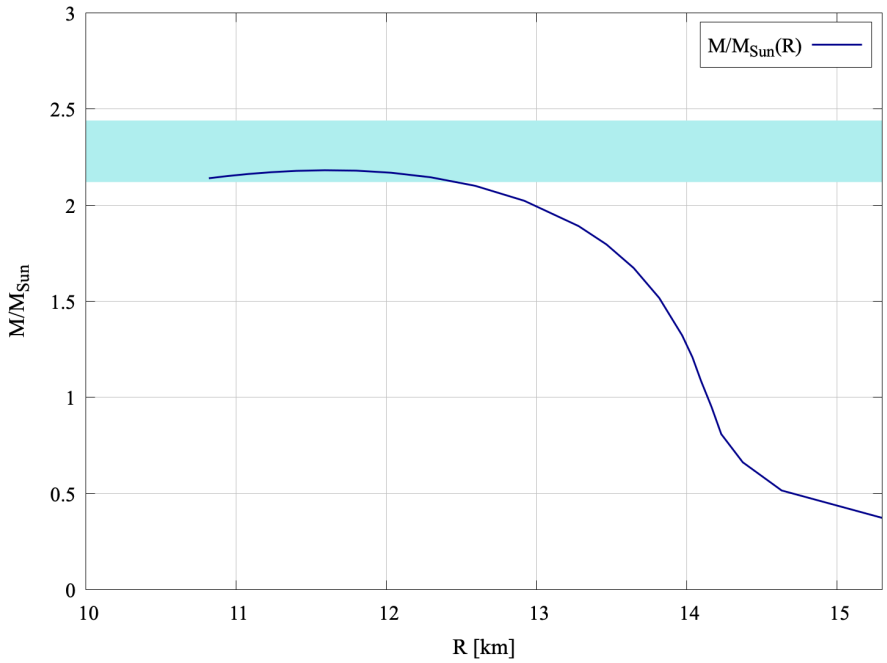

Figure 5.5. Mass-radius diagram for the EOS discussed in the text and plotted in Fig 5.4. The horizontal band indicates the constraints from analysis of PSR J2215+5135 [21].

5.2 Strange matter case

As it has been explained in chapter 3 the first hyperon to appear should be Σ^-, mainly for its negative charge that would favor its onset before that of Λ even if it has a higher mass. Nevertheless, in this work we study the strange matter considering the presence of hyperon Λ. The main reason of interest for examining the case with this specific strange baryon is that the Λ can be observed in hypernuclei, thanks, for instance, to the kaon electro-production process in which an electron scatters off a nucleus of mass number A. The hadronic final state comprises a K^+ meson and the recoiling hypernucleus, resulting from the replacement of a proton with a Λ in the target nucleus [22]. Thus, the experimental studies of hypernuclear dynamics could provide important informations about strong interactions in the strange sector and so possible constraints on Λ hyperon couplings. Instead experimental data of Σ-hypernuclei are scarce and unclear.
By including only the Lambda strange baryon in addition to nucleons in our model, the equations of motion (3.24)-(3.26) of the meson fields, rearranging some terms, become

$$\begin{aligned} m_\sigma^2\sigma = &\sum_{i=p,n} \frac{1}{\pi^2} g_\sigma \int_0^{k_{F_i}} k^2 dk \frac{m_N^*}{\sqrt{k^2 + m_N^{*2}}^2} \\ &+ \frac{1}{\pi^2} g_{\Lambda\sigma} \int_0^{k_{F_\Lambda}} k^2 dk \frac{m_\Lambda - g_{\Lambda\sigma}\sigma}{\sqrt{k^2 + (m_\Lambda - g_{\Lambda\sigma}\sigma)^2}} \\ &- b m_N g_\sigma^3 \sigma^2 - c g_\sigma^4 \sigma^3 \end{aligned} \tag{5.14}$$

$$m_\omega^2 \omega^0 = g_\omega (n_p + n_n) + g_{\Lambda\omega} n_\Lambda \tag{5.15}$$

$$m_\rho^2 \rho^{03} = \frac{1}{2} g_\rho (n_p - n_n). \tag{5.16}$$

It should be noted that, since Λ has zero isospin 3-component, the equation of motion of vector meson ρ^{03} does not change, unlike the other two. Now the total baryon density is clearly $n_B = n_p + n_n + n_\Lambda$. From the equation (5.14) we can also define the effective mass of Lambda

$$m_\Lambda^* = m_\Lambda - g_{\Lambda\sigma}\sigma, \tag{5.17}$$

which is related to that of nucleons by expression

$$\frac{m_\Lambda - m_\Lambda^*}{m_N - m_N^*} = \frac{g_{\Lambda\sigma}}{g_\sigma}. \tag{5.18}$$

The above equation shows how the presence of hyperon influences through the interaction with the scalar meson the nucleons and the interaction of the latter with the same meson affects in turn Λ.
By using the equations of motion (5.14)-(5.16) and the usual relations of Fermi momentum and effective nucleon mass, we obtain the equation of state (3.27)-(3.28) for the specific Λ case as function of total baryon density

$$\begin{aligned}
\epsilon(n_p, n_n, n_\Lambda) &= \tfrac{1}{2}\tfrac{m_\sigma^2}{g_\sigma^2}(m_N - m_N^*)^2 + \tfrac{1}{8}\tfrac{g_\rho^2}{m_\rho^2}(n_p - n_n)^2 \\
&+ \tfrac{1}{2}\tfrac{1}{m_\omega^2}[g_\omega(n_p + n_n) + g_{\Lambda\omega} n_\Lambda]^2 \\
&+ \tfrac{b}{3} m_N (m_N - m_N^*)^3 + \tfrac{c}{4}(m_N - m_N^*)^4 + \\
&+ \tfrac{1}{\pi^2}\textstyle\sum_{i=p,n} \int_0^{k_{F_i}} k^2 dk \sqrt{|\mathbf{k}|^2 + m_N^{*2}} \\
&+ \tfrac{1}{\pi^2}\int_0^{k_{F_\Lambda}} k^2 dk \sqrt{|\mathbf{k}|^2 + m_\Lambda^{*2}},
\end{aligned} \tag{5.19}$$

and

$$\begin{aligned}
P(n_p, n_n, n_\Lambda) &= -\tfrac{1}{2}\tfrac{m_\sigma^2}{g_\sigma^2}(m_N - m_N^*)^2 + \tfrac{1}{8}\tfrac{g_\rho^2}{m_\rho^2}(n_p - n_n)^2 \\
&+ \tfrac{1}{2}\tfrac{1}{m_\omega^2}[g_\omega(n_p + n_n) + g_{\Lambda\omega} n_\Lambda]^2 \\
&- \tfrac{b}{3} m_N (m_N - m_N^*)^3 - \tfrac{c}{4}(m_N - m_N^*)^4 + \\
&+ \tfrac{1}{3\pi^2}\textstyle\sum_{i=p,n} \int_0^{k_{F_i}} dk \frac{k^4}{\sqrt{k^2 + m_N^{*2}}} \\
&+ \tfrac{1}{3\pi^2}\int_0^{k_{F_\Lambda}} dk \frac{k^4}{\sqrt{k^2 + m_\Lambda^{*2}}}.
\end{aligned} \tag{5.20}$$

The terms in addition to the nonstrange case are those on the second and fifth rows of the above equations.
In order to calculate numerically the EOS we still use 1P computational code but now it also takes as input the hyperon coupling constants. In the program there is a Boolean variable that allows to easily switch from the case without Λ to that in

which the hyperon is present.
The hyperon couplings are not determined by ground state properties of nuclear matter and the current constraints from experimental data are considerable uncertain even at the nuclear density and become even more so at higher densities. In view of this uncertainty we use in this work [12]

$$\left(\frac{g_{\Lambda\sigma}}{g_\sigma}\right)^2 = \left(\frac{g_{\Lambda\omega}}{g_\omega}\right)^2 = \frac{2}{3} \quad , \quad g_{\Lambda\rho} = 0. \tag{5.21}$$

The ratio between the hyperon-scalar meson and nucleon-scalar meson couplings are evaluated on the basis of a semplified quark model by analyzing the strange and non-strange quark content of the baryons. In this quark model the scalar meson σ describing the intermediate range force between baryons is modelled as a quark-antiquark system $\sigma = (u\overline{u} + d\overline{d})/\sqrt{2}$, which is essentialy the number operator of non-strange quarks. Since nucleons contain three nonstrange quarks, while the Λ only contain two, it follows that the coupling constants of the Λ-nucleon interaction mediated by the σ-meson is 2/3 of the corresponding nucleon-nucleon coupling constant [23]. For semplicity, we also extend the concept to coupling with ω-meson taking the same ratio value, whereas the coupling constant with vector meson ρ is zero because Lambda has not isospin 3-component and so does not interact with it. With this configuration we consider the strange baryon matter in general β-equilibrium as discussed in section 3.0.1. The matter composition is shown in Fig. 5.6.

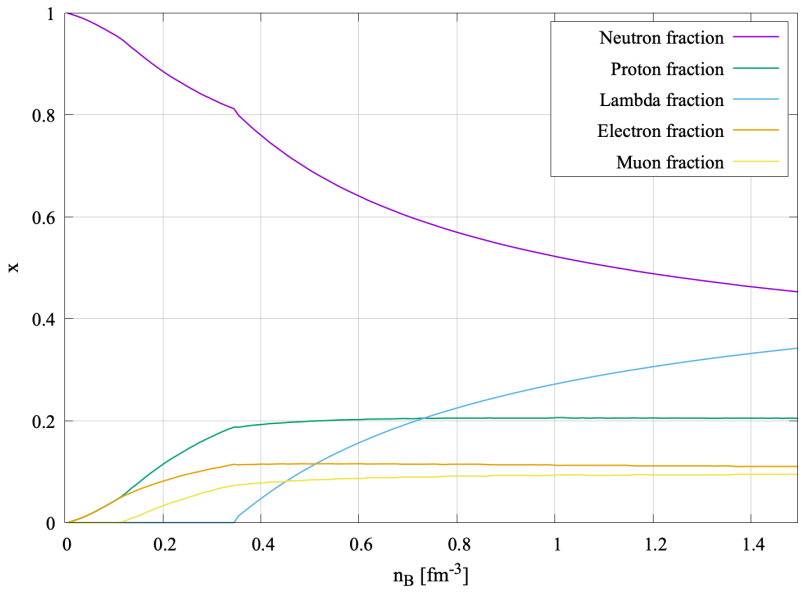

Figure 5.6. Fractions of the different matter constituents in beta equilibrium as a function of the total baryon density.

The onset of the Λ occurs when the effective nucleon chemical potential equals or exceeds that of the Lambda, i.e. it satisfies the threshold equation

$$\mu_N^* \geq g_{\Lambda\omega}\omega^0 + m_\Lambda^*. \tag{5.22}$$

For our model this condition starts to be verified at density $n_B \sim 0.35$ fm^{-3} that is about twice the saturation density as expected in recent literature and discussed in chapter 3. Regarding the charge neutrality condition, it remains as in nonstrange case $n_p = n_e + n_\mu$ because the Λ has zero electrical charge. For this reason, it is not possible to observe the strong deleptonization discussed in chapter 3, which occurs when we consider negatively charged strange baryons that can directly replace leptons in the neutral charge balance. Despite this, a reduction in electron and muon concentrations can be noted ($\sim 30\%$) as a consequence of the decrease in the proton fraction for the conversion of part of neutrons into hyperons.
Following the same approach of the previous chapter, also for this case, we can recast the equation of state in the form

$$\begin{aligned} P(\epsilon) &= \epsilon - \frac{m_\sigma^2}{g_\sigma^2}(m_N - m_N^*)^2 - \frac{2}{3}bm_N(m_N - m_N^*)^3 - \frac{c}{2}(m_N - m_N^*)^4 + \\ &+ \frac{1}{3\pi^2}\sum_{i=p,n}\int_0^{k_{F_i}} dk \frac{k^4}{\sqrt{k^2+m_N^{*2}}} \\ &+ \frac{1}{3\pi^2}\int_0^{k_{F_\Lambda}} dk \frac{k^4}{\sqrt{k^2+m_\Lambda^{*2}}} \\ &- \frac{1}{\pi^2}\sum_{i=p,n}\int_0^{k_{F_i}} k^2 dk \sqrt{|\mathbf{k}|^2 + m_N^{*2}} \\ &- \frac{1}{\pi^2}\int_0^{k_{F_\Lambda}} k^2 dk \sqrt{|\mathbf{k}|^2 + m_\Lambda^{*2}}, \end{aligned} \tag{5.23}$$

where the only additional terms compared to (5.13) are the Lambda integrals since the parts related to the vector mesons vanish in the semplifications that lead to the above equation. The trend of the pressure as a function of energy density for strange matter is plotted in Fig. 5.7.

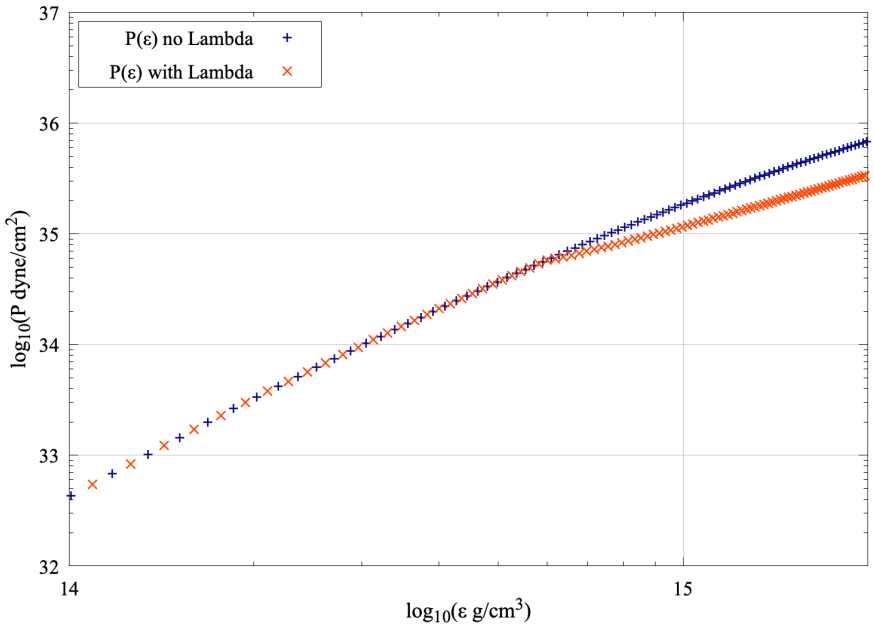

Figure 5.7. Comparison of the two equations of state with and without the hyperon Λ.

In the graph the EOS of nonstrange matter is also present in order to show how the pressure decreases when hyperon appears. The conversion of most energetic neutrons into massive and slowly moving hyperon relieves the Fermi pressure exerted by the baryons and make the equation of state softer, as it is illustred in the figure. It should be stressed that, even if the graph 5.7 does not show the region at lower densities to emphasize the pressure difference between the two situations under examination, also in strange matter case we substitute the computed equation of state with crust EOS at densities $< n_0$. The deviation between the two trends starts, of course, at ~ 0.35 fm^{-3} that corresponds to energy density and pressure values respectively of $\epsilon \sim 6 \times 10^{14}$ g/cm^3 and $P \sim 6 \times 10^{34}$ dyne/cm^2. The maximum appreciable difference occurs at $\epsilon \sim 2 \times 10^{15}$ g/cm^3 where the pressure drops from $P \sim 7 \times 10^{35}$ to $P \sim 3 \times 10^{35}$ dyne/cm^2. It is practically reduced by fifty percent. As a consequence, the gravitational mass of the star, expecially the maximum one, is substantially lowered. The comparison of the mass-radius relation for strange matter, numerically evaluated always with the 2P computational code, and nonstrange matter is shown in Fig. 5.8.

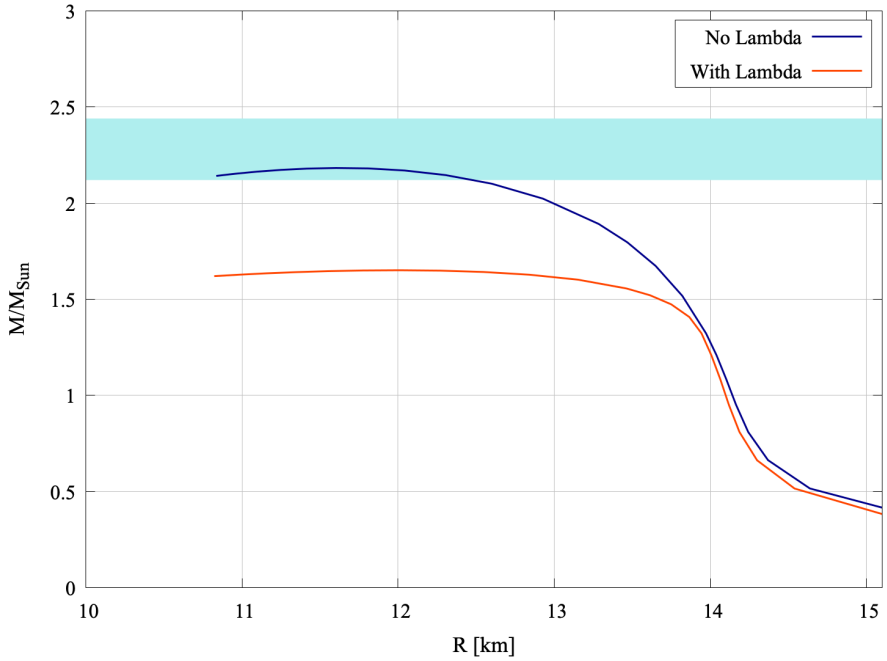

Figure 5.8. Comparison of the two mass-radius relations for the EOS including Λ or not. Even in this case as in Fig. 5.5, the horizontal band denotes the experimental limits from analysis of PSR J2215+5135.

The maximum mass for the case with hyperon, reached at $R \sim 12$ km, is $\sim 1.65\, M_\odot$ that is evidently not compatible with recent observational data, as can be observed from the graph.

Chapter 6

Conclusions

In this work we discussed the hyperon puzzle, i.e. the difficulty to conciliate the measured masses of neutron stars with the presence of hyperons in their inner cores. First of all, we briefly reviewed the evolution and structure of a neutron star. Then we built a theoretical framework for our study, illustrating the main properties of nuclear matter and introducing the relativistic mean field theory. Thus we discussed the $\sigma\omega\rho$ model used to obtain the equation of state describing the stellar matter. This was first studied for a system that includes only nucleons and later generalized to the hyperons Λ, Σ and Ξ. In both cases we have pointed out the conditions for the equilibrium between the nuclear components of stellar matter, i.e. the conditions of charge neutrality and β-stability. Lastly, to complete this theoretical scheme, we treated the Tolman-Oppenheimer-Volkoff equations necessary to examine the internal structure of neutron stars and to obtain the characteristic mass-radius relationship that is fundamental to show the hyperonization effect on hadronic star mass.

After all these theoretical considerations, we presented our numerical results evaluated thanks to two *Fortran* computational code implemented to calculate the EOS and TOV equations in nonstrange and strange matter cases. In the latter situation we considered only the presence of the hyperon Λ. On a personal computer of intermediate level, the typical CPU time required for the strange EOS computation is of ~ 19 s, while for the other calculations is about two seconds or less.

Comparing the trend of the pressure and the mass-radius relation has been possible to observe as even if the model used is much simplified it clearly illustrated the hyperon puzzle. Indeed, when the Λ appears the pressure drops and consequently the limiting mass also does reaching a value not compatible with recent experimental data. We obtained a mass reduction of $\sim 24\%$.

The choice to use relativistic mean field theory is in keeping with a lot of works of literature. However, it should be stressed that even in the most complete models the results obtained are ambiguous and not accurate. This is because, as mentioned in the work, the relativistic approach, even if it is causal consistent by construction, is based on a somewhat simplified dynamics and the parameters that characterize the models are not fully constrained by available experimental data. Moreover, it is affected by the uncertainty related to the use of the mean field approximation, which fails in strongly correlated systems.

An alternative approach is to use non relativistic nuclear many-body theory. The dynamics description is more realistic but the models of this theory suffer from the limitations ineherent in the non relativistic approximation, that can lead to a causality violation, determined by stiffness of the equation of state in the infinite density limit.
From all these considerations it is clear that the hyperon puzzle is still shrouded in uncertainty and far from being fully understood. The difficult solution of this problem is currently a subject of very active experimental and theoretical research. There are several possible mechanisms that could produce the additional repulsion needed to make the equation of state stiffer and therefore the maximum mass compatible with the current observational limits. For the relativistic approach, for instance, there is that of the interaction between only hyperons with the exchange of a hidden strangeness vector meson [24] or that in which the repulsion in the hyperon-hyperon interaction is reached by introducing density dependent couplings [25]. Another interesting hypothesis is to consider the pressure anisotropy in the core of hadronic stars [26]. As regards the non-relativistic approach, the mechanism most often considered is that of three-body forces involving one or more hyperons with the introduction also here of a phenomenological dependence of coupling constants on baryon density [27]. However none of these has so far led to completely satisfactory results.

Appendix A

β equilibrium

As mentioned in section (3.0.1) at densities in the vicinity of nuclear matter density, charge-neutral matter of a cold star is a system basically composed of neutrons and a small admixture of protons with equal number of electrons, once equilibrium with respect to β-decay, and its inverse process,

$$n \to p + e^- + \overline{\nu}_e \iff p + e^- \to n + \nu_e \tag{A.1}$$

has been reached.
It should be noted that, assuming neutrinos to be massless, the electron capture process is energetically favorable only when the electron energy becomes equal to the neutron-proton mass difference

$$\Delta m = m_n - m_p = 939.565 - 938.272 = 1.293\,\mathrm{MeV}. \tag{A.2}$$

Consequently, the value of n_e at which inverse β-decay sets in can be estimated from

$$\sqrt{k_{Fe}^2 + m_e^2} = \Delta m, \tag{A.3}$$

where $k_{Fe}^2 = (3\pi^2 n_e)^{1/3}$, leading to

$$n_e = \frac{1}{3\pi^2}(\Delta m^2 - m_e^2)^{3/2} \approx 7 \times 10^{30}\,\mathrm{cm}^{-3}. \tag{A.4}$$

In order to extrapolate the equation of chemical potential equilibrium (3.11) it is important remark that weak interaction processes (A.1) conserve baryon number, n_B, and electric charge but not isospin quantum number by modifying the particle fractions in the matter.
For any given value of n_B, the ground state is found by minimization of the total energy density of the system, $\epsilon(n_p, n_n, n_e)$, n_p and n_n being the proton and neutron density, respectively, with the constraints $n_B = n_p + n_n$, conservation of baryon number, and $n_p = n_e$, charge neutrality.
Let us define the function

$$F(n_p, n_n, n_e) = \epsilon(n_p, n_n, n_e) + \lambda_B(n_B - n_p - n_n) + \lambda_Q(n_p - n_e) \tag{A.5}$$

where ϵ is the energy density, while λ_B and λ_Q are Lagrange multipliers.
The minimum of F corrisponds to the values on n_p, n_n and n_e satisfying the conditions

$$\frac{\partial F}{\partial n_p} = \frac{\partial F}{\partial n_n} = 0\,,\ \frac{\partial F}{\partial n_e} = 0 \tag{A.6}$$

as well as the additional constraints

$$\frac{\partial F}{\partial \lambda_B} = \frac{\partial F}{\partial \lambda_Q} = 0. \tag{A.7}$$

From the definition of chemical potential of the particles of species i $(i = p, n, e)$

$$\mu_i = \left(\frac{\partial E}{\partial N_i}\right)_V = \left(\frac{\partial \epsilon}{\partial n_i}\right)_V \tag{A.8}$$

it follows that Eqs. (A.6) imply

$$\begin{aligned} &\mu_p - \lambda_B + \lambda_Q = 0, \\ &\mu_n - \lambda_B = 0, \\ &\mu_e - \lambda_Q = 0. \end{aligned} \tag{A.9}$$

Finally, rearranging the terms, the above equations lead to the condition of chemical equilibrium

$$\begin{aligned} \mu_n - \mu_p - \mu_e &= 0 \\ \Rightarrow \mu_n &= \mu_p + \mu_e. \end{aligned} \tag{A.10}$$

Appendix B

Weak and stationary limit of Einstein field equations

Consider a non-relativistic particle in a weak and stationary gravitational field. Restoring the constant c, the particle proper time is τ/c. Since $v << c$, it follows that

$$\frac{dx^i}{dt} << c \qquad \rightarrow \qquad \frac{dx^i}{d\tau} << \frac{cdt}{d\tau} = \frac{dx^0}{d\tau}. \tag{B.1}$$

Thus the geodesic equation (4.14) becomes

$$\frac{d^2x^\mu}{d\tau^2} + \Gamma^\mu_{00}\left(\frac{dx^0}{d\tau}\right)^2 = 0. \tag{B.2}$$

From the expressions of the affine connections in terms of $g_{\mu\nu}$, Eq. (4.13), we find that

$$\Gamma^\mu_{00} = \frac{1}{2}g^{\mu\sigma}(2g_{0\sigma,0} - g_{00,\sigma}). \tag{B.3}$$

In addition, if the field is stationary $g_{0\sigma,0} = 0$, and

$$\Gamma^\mu_{00} = -\frac{1}{2}g^{\mu\sigma}g_{00,\sigma}. \tag{B.4}$$

The weak field limit can be interpreted as that we can choose a reference frame in which the metric is nearly flat, therefore

$$g_{\mu\nu} = \eta_{\mu\nu} + h_{\mu\nu}, \qquad |h_{\mu\nu}| << 1, \tag{B.5}$$

where $h_{\mu\nu}$ is a small perturbation of the flat metric. Since we are interest in first order terms in $h_{\mu\nu}$ we can raise and lower its indices with flat metric $\eta^{\mu\nu}$. For example

$$h^\lambda{}_\nu = g^{\lambda\rho}h_{\rho\nu} \sim \eta^{\lambda\rho}h_{\rho\nu} + O(h^2_{\mu\nu}) \tag{B.6}$$

Substituting eq. (B.5) into eq. (B.4), and retain only the terms up to first order in $h_{\mu\nu}$ we find

$$\Gamma^\mu_{00} \sim -\frac{1}{2}\eta^{\mu\sigma}\frac{\partial h_{00}}{\partial x^\sigma} \tag{B.7}$$

that put in geodesic equation leads to

$$\begin{aligned} \frac{d^2x^\mu}{d\tau^2} &= \frac{1}{2}\eta^{\mu\alpha}\frac{\partial h_{00}}{\partial x^\alpha}\left(\frac{cdt}{d\tau}\right)^2 \\ \Rightarrow \frac{d^2\mathbf{x}}{d\tau^2} &= \frac{1}{2}\boldsymbol{\nabla} h_{00}\left(\frac{cdt}{d\tau}\right)^2. \end{aligned} \tag{B.8}$$

The time-component vanishes because we have assumed that the field is stationary and so $\frac{\partial h_{00}}{\partial t} = 0$.
If we rescale the time coordinate according to $cdt/d\tau = 1$ we find

$$\frac{d^2\mathbf{x}}{dt^2} = \frac{c^2}{2}\boldsymbol{\nabla} h_{00}. \tag{B.9}$$

Remembering that the corresponding Newtonian equation is

$$\frac{d^2\mathbf{x}}{dt^2} = -\boldsymbol{\nabla}\phi, \tag{B.10}$$

where ϕ is the gravitational potential given by Poisson equation (4.3), we see that it must be

$$h_{00} = -2\frac{\phi}{c^2} + \text{const.} \tag{B.11}$$

If the field is stationary and spherically symmetric, the newtonian potential is

$$\phi = -\frac{GM}{r}, \tag{B.12}$$

and if require that h_{00} vanishes at infinity, the constant must be zero and eq. (B.11) leads to

$$h_{00} = -2\frac{\phi}{c^2} \Rightarrow g_{00} = -(1 + 2\frac{\phi}{c^2}). \tag{B.13}$$

Thus we have demonstrated that in weak field limit the geodesic equations reduce to the newtonian law of gravitation.
Now we can show that a classical mass-energy distribution will curve spacetime in a way that produces the gravitational field predicted by Newton's law of gravity so that

$$G_{\mu\nu} = \left(R_{\mu\nu} - \frac{1}{2}g_{\mu\nu}R\right) = kT_{\mu\nu} \tag{B.14}$$

contains the Poisson equation (4.3). In this way we will define the constant k.
If the field is weak, matter will behave non-relativistically, i.e. $T_{00} \sim \rho c^2$. Moreover, in this limit we have

$$|T_{ij}| << |T_{00}|, \qquad i,j = 1,3\,, \tag{B.15}$$

and therefore

$$|G_{ij}| << |G_{00}|, \qquad i,j = 1,3\,, \tag{B.16}$$

hence

$$R_{ij} \simeq \frac{1}{2}g_{ij}R. \tag{B.17}$$

Since $g_{ij} \simeq \eta_{ij}$ we obtain

$$R_{kk} \simeq -\frac{1}{2}R, \qquad k = 1, 3 \tag{B.18}$$

as a consequence

$$\begin{gathered} R = g^{\mu\nu}R_{\mu\nu} \simeq \eta_{\mu\nu}R_{\mu\nu} = R_{00} - \sum_k R_{kk} = R_{00} + \frac{3}{2}R, \\ \Rightarrow R \simeq -2R_{00}. \end{gathered} \tag{B.19}$$

The result of all these above considerations is that Eq. (B.14) takes the form ($g_{00} = \eta_{00} = 1$)

$$\begin{gathered} R_{00} - \frac{1}{2}R = kT_{00} \\ \Rightarrow R_{00} = \frac{k\rho}{2}. \end{gathered} \tag{B.20}$$

But R_{00} is the contraction $R^{\mu}_{0\mu0}$. Recalling the expression of Riemann tensor (4.12), we have

$$R_{00} = R^{\mu}_{0\mu0} = \partial_\mu\Gamma^{\mu}_{00} - \partial_0\Gamma^{\mu}_{0\mu} + \Gamma^{\alpha}_{00}\Gamma^{\mu}_{\alpha\mu} - \Gamma^{\alpha}_{0\mu}\Gamma^{\mu}_{\alpha0}. \tag{B.21}$$

The second term is a time derivarite and so vanishes because the field is static. We are interested in expressions linear in the metric and, by definition, the affine connections are already first-order in g_{ij}. Thus the third and fourth terms are second-order in the metric and so negligible.
What remains is

$$R_{00} = \partial_\mu\Gamma^{\mu}_{00}. \tag{B.22}$$

Combining (B.7), (B.20) and (B.22), we find

$$\eta^{\mu\sigma}\partial_\mu\partial_\sigma h_{00} = -k\rho. \tag{B.23}$$

Since off-diagonal entries of the Minkowski metric matrix are zero and the gravitational field is static, we have

$$\begin{gathered} -\partial_1\partial_1 h_{00} - \partial_2\partial_2 h_{00} - \partial_3\partial_3 h_{00} = -k\rho \\ \Rightarrow \boldsymbol{\nabla}^2 h_{00} = k\rho. \end{gathered} \tag{B.24}$$

We have seen that we can relate geodesic equation to Newton's second law if we require $h_{00} = -2\frac{\phi}{c^2}$. Now we can simplify (B.24) into

$$\boldsymbol{\nabla}^2\phi = -k\frac{c^2}{2}\rho, \tag{B.25}$$

and setting the constant

$$k = -\frac{8\pi G}{c^2} \tag{B.26}$$

we find the Poisson equation (4.3).
Finally, putting $c = 1$, the Einstein equation (B.14) reads

$$G_{\mu\nu} = -8\pi G T_{\mu\nu}. \tag{B.27}$$

Bibliography

[1] J. R. Oppenheimer and G. M. Volkoff. "On Massive Neutron Cores". In: *Phys. Rev.* 55 (4 1939), pp. 374–381. doi: 10.1103/PhysRev.55.374. url: https://link.aps.org/doi/10.1103/PhysRev.55.374.

[2] Subrahmanyan Chandrasekhar. "The maximum mass of ideal white dwarfs". In: *Astrophys. J.* 74 (1931), pp. 81–82. doi: 10.1086/143324.

[3] VA Ambartsumyan and GS Saakyan. "The degenerate superdense gas of elementary particles". In: *Soviet Astronomy* 4 (1960), p. 187.

[4] N. K. Glendenning. *Compact stars: Nuclear physics, particle physics, and general relativity*. Springer, 2000.

[5] Omar Benhar and Alessandro Lovato. "Perturbation Theory of Nuclear Matter with a Microscopic Effective Interaction". In: *Phys. Rev. C* 96.5 (2017), p. 054301. doi: 10.1103/PhysRevC.96.054301. arXiv: 1706.00760 [nucl-th].

[6] Anis ben Ali Dadi. "Parametrization of the Relativistic ($\sigma - \omega$) Model for Nuclear Matter". In: *Phys. Rev. C* 82 (2010), p. 025203. doi: 10.1103/PhysRevC.82.025203. arXiv: 1005.2030 [nucl-th].

[7] B. D. DAY. "Elements of the Brueckner-Goldstone Theory of Nuclear Matter". In: *Rev. Mod. Phys.* 39 (4 1967), pp. 719–744. doi: 10.1103/RevModPhys.39.719. url: https://link.aps.org/doi/10.1103/RevModPhys.39.719.

[8] Bernard ter Haar and Rudi Malfliet. "Pion production, pion absorption, and nucleon properties in dense nuclear matter: Relativistic Dirac-Brueckner approach at intermediate and high energies". In: *Phys. Rev. C* 36 (4 1987), pp. 1611–1620. doi: 10.1103/PhysRevC.36.1611. url: https://link.aps.org/doi/10.1103/PhysRevC.36.1611.

[9] R. Brockmann and R. Machleidt. "Relativistic nuclear structure. I. Nuclear matter". In: *Phys. Rev. C* 42 (5 1990), pp. 1965–1980. doi: 10.1103/PhysRevC.42.1965. url: https://link.aps.org/doi/10.1103/PhysRevC.42.1965.

[10] J. D. Walecka. "A Theory of highly condensed matter". In: *Annals Phys.* 83 (1974), pp. 491–529. doi: 10.1016/0003-4916(74)90208-5.

[11] J. Boguta and A. R. Bodmer. "Relativistic Calculation of Nuclear Matter and the Nuclear Surface". In: *Nucl. Phys. A* 292 (1977), pp. 413–428. doi: 10.1016/0375-9474(77)90626-1.

[12] N. K. Glendenning. "Neutron Stars Are Giant Hypernuclei?" In: *Astrophys. J.* 293 (1985), pp. 470–493. doi: 10.1086/163253.

[13] S. I. A. Garpman, N. K. Glendenning, and Y. J. Karant. "THERMODYNAMIC BEHAVIOR OF NONSTRANGE BARYONIC MATTER". In: *Nucl. Phys. A* 322 (1979), pp. 382–396. DOI: 10.1016/0375-9474(79)90433-0.

[14] Shmuel Balberg, Itamar Lichtenstadt, and Gregory B. Cook. "Roles of hyperons in neutron stars". In: *Astrophys. J. Suppl.* 121 (1999), p. 515. DOI: 10.1086/313196. arXiv: astro-ph/9810361.

[15] Valeria Ferrari, Leonardo Gualtieri, and Paolo Pani. *General Relativity and its Applications*. CRC Press, Taylor & Francis Group, 2020. ISBN: 978-0-367-62532-0.

[16] Richard C. Tolman. "Static Solutions of Einstein's Field Equations for Spheres of Fluid". In: *Phys. Rev.* 55 (4 1939), pp. 364–373. DOI: 10.1103/PhysRev.55.364. URL: https://link.aps.org/doi/10.1103/PhysRev.55.364.

[17] C. J. Horowitz and Brian D. Serot. "The Relativistic Two Nucleon Problem in Nuclear Matter". In: *Nucl. Phys. A* 464 (1987). [Erratum: Nucl.Phys.A 473, 760 (1987)], p. 613. DOI: 10.1016/0375-9474(87)90370-8.

[18] Sanjay Reddy and Madappa Prakash. "Neutrino scattering in a newly born neutron star". In: *Astrophys. J.* 478 (1997), pp. 689–700. DOI: 10.1086/303804. arXiv: astro-ph/9610115.

[19] Pawel Danielewicz, Roy Lacey, and William G. Lynch. "Determination of the equation of state of dense matter". In: *Science* 298 (2002), pp. 1592–1596. DOI: 10.1126/science.1078070. arXiv: nucl-th/0208016.

[20] C. P. Lorenz, D. G. Ravenhall, and C. J. Pethick. "Neutron star crusts". In: *Phys. Rev. Lett.* 70 (4 1993), pp. 379–382. DOI: 10.1103/PhysRevLett.70.379. URL: https://link.aps.org/doi/10.1103/PhysRevLett.70.379.

[21] Manuel Linares, Tariq Shahbaz, and Jorge Casares. "Peering into the dark side: Magnesium lines establish a massive neutron star in PSR J2215+5135". In: *Astrophys. J.* 859.1 (2018), p. 54. DOI: 10.3847/1538-4357/aabde6. arXiv: 1805.08799 [astro-ph.HE].

[22] Omar Benhar. "Extracting Hypernuclear Properties from the $(e, e'K^+)$ Cross Section". In: (June 2020). arXiv: 2006.12084 [nucl-th].

[23] Steven A. Moszkowski. "Energy of neutron-star matter". In: *Phys. Rev. D* 9 (6 1974), pp. 1613–1625. DOI: 10.1103/PhysRevD.9.1613. URL: https://link.aps.org/doi/10.1103/PhysRevD.9.1613.

[24] S. Weissenborn, D. Chatterjee, and J. Schaffner-Bielich. "Hyperons and massive neutron stars: Vector repulsion and SU(3) symmetry". In: *Phys. Rev. C* 85 (6 2012), p. 065802. DOI: 10.1103/PhysRevC.85.065802. URL: https://link.aps.org/doi/10.1103/PhysRevC.85.065802.

[25] K. A. Maslov, E. E. Kolomeitsev, and D. N. Voskresensky. "Relativistic Mean-Field Models with Scaled Hadron Masses and Couplings: Hyperons and Maximum Neutron Star Mass". In: *Nucl. Phys. A* 950 (2016), pp. 64–109. DOI: 10.1016/j.nuclphysa.2016.03.011. arXiv: 1509.02538 [astro-ph.HE].

[26] A. Rahmansyah et al. "Anisotropic neutron stars with hyperons: implication of the recent nuclear matter data and observations of neutron stars". In: *Eur. Phys. J. C* 80.8 (2020), p. 769. DOI: 10.1140/epjc/s10052-020-8361-4.

[27] Isaac Vidana et al. "Estimation of the effect of hyperonic three-body forces on the maximum mass of neutron stars". In: *EPL* 94.1 (2011), p. 11002. DOI: 10.1209/0295-5075/94/11002. arXiv: 1006.5660 [nucl-th].

[28] S. L. Shapiro and S. A. Teukolsky. *Black holes, white dwarfs, and neutron stars: The physics of compact objects*. 1983. ISBN: 978-0-471-87316-7.

[29] Weber F. *Pulsars as Astrophysical Laboratories for Nuclear and Particle Physics*. 1999.

[30] Omar Benhar. *The Structure of Compact Stars*. 2017.

[31] Diego Lonardoni et al. "Hyperon Puzzle: Hints from Quantum Monte Carlo Calculations". In: *Phys. Rev. Lett.* 114.9 (2015), p. 092301. DOI: 10.1103/PhysRevLett.114.092301. arXiv: 1407.4448 [nucl-th].

[32] H. T. Cromartie et al. "Relativistic Shapiro delay measurements of an extremely massive millisecond pulsar". In: *Nature Astron.* 4.1 (2019), pp. 72–76. DOI: 10.1038/s41550-019-0880-2. arXiv: 1904.06759 [astro-ph.HE].

[33] Isaac Vidana. "Hyperons and Neutron Stars". In: *PoS* MPCS2015 (2016), p. 027. DOI: 10.22323/1.262.0027.

[34] J. Schaffner-Bielich. "Strangeness in Compact Stars". In: *Nucl. Phys. A* 835 (2010). Ed. by Benjamin F. Gibson et al., pp. 279–286. DOI: 10.1016/j.nuclphysa.2010.01.203. arXiv: 1002.1658 [nucl-th].